

ExtremalDep: Modelling extremal dependence in high-dimensional extremes

Boris Beranger¹  and Simone A. Padoan² 

¹*School of Mathematics and Statistics, UNSW Data Science Hub (uDASH), UNSW Sydney*

E-mail: B.Beranger@unsw.edu.au

²*Department of Decisions Sciences, Bocconi University*

E-mail: Simone.Padoan@unibocconi.it

December 19, 2024

Abstract

From environmental sciences to finance, there are growing needs for assessing the risk of more extreme events than those observed. Extrapolating extreme events beyond the range of the data is not obvious and requires advanced tools based on extreme value theory. Furthermore, the complexity of risk assessments often requires the inclusion of multiple variables. Extreme value theory provides very important tools for the analysis of multivariate or spatial extreme events, but these are not easily accessible to professionals without appropriate expertise. This article provides a minimal background on multivariate and spatial extremes and gives simple yet thorough instructions to analyse high-dimensional extremes using the R package **ExtremalDep**. After briefly introducing the statistical methodologies, we focus on road testing the package's toolbox through several real-world applications.

Keywords: Angular measure, Air pollution, Environmental data analysis, Exchange rates, Extremal coefficient, Extreme sets, Heat Waves, Max-stable processes, Multivariate generalized extreme-value distribution, Pickands dependence function, Quantile regions.

1 Introduction

In many applied fields, ranging from environmental sciences, finance to insurance, it is crucial to be able to assess the risk of more extreme events than those observed, with the goal to assess future catastrophes (e.g., a global financial crisis or large monetary losses due to natural hazards). The aim is ultimately to disclose the uncertainty about such extreme events to decision makers in order to carefully plan mitigation strategies. Extrapolating to extreme events lying beyond the range of N existing data observations, is of high importance in risk management. The solution to this extreme value problem is not obvious since the occurrence probabilities (p) in the extrapolation regime are likely to be smaller than $1/N$ and therefore none of the observed data points exceed the desired event. Extreme Value Theory (EVT) provides a framework to develop probabilistic models and statistical methods for modelling extreme events. For a basic introduction, see for example [Beirlant et al. \(2004\)](#), [de Haan and Ferreira \(2006\)](#) and [Falk et al. \(2010\)](#).

In the univariate case, the theory and practice is mature with a significant number of packages available on the Comprehensive R Archive Network (CRAN), forming an extensive set of tools. Examples include **ismev** (Heffernan and Stephenson, 2018), **evd** Stephenson (2002), **evdbayes** (Stephenson and Ribatet, 2023), **extRemes** (Gilleland and Katz, 2016) and **ExtremeRisks** (Padoan and Stupfler, 2020) to name a few. In practice, however, multiple variables are often observed. For instance, rainfall, temperature and wind may be observed at several locations spread across a region and contribute to the economic losses due to bad weather conditions; high pollution level is the result of a combination of multiple pollutants exceeding safety thresholds, etc. Focusing on multivariate and spatial problems, statistical methodologies for the analysis of high-dimensional extremes and their software implementation are less developed. The *extremal dependence* refers to the dependence structure behind multivariate extreme value distributions or the finite-dimensional distribution of stochastic processes for extremes. It is an infinite-dimensional (nonparametric) object subject to restrictive conditions, resulting in a complex formulation of the overall multivariate distribution and inferential challenges. The literature on high-dimensional extremes covers several topics including multivariate extremes (e.g. Beranger and Padoan, 2015), spatial extremes (e.g Davison et al., 2012; de Fondeville and Davison, 2018), graphical models (Engelke and Hitz, 2020) and time series (e.g. Davis et al., 2011), and is remains nowadays a vibrating research field with a number of ongoing new results. These have produced useful R packages such as **ExtremalDep** (Beranger et al., 2024), **mev** (Belzile et al., 2022), **SpatialExtremes** (Ribatet, 2022), **mvPot** (de Fondeville and Belzile, 2021), **RandomFields**, **graphicalExtremes** Engelke et al. (2024) and **extremogram** (Frolova and Cribben, 2016). A review and comparison of statistical software for modelling extremes is presented in Belzile et al. (2023).

Most of the existing packages designed to analyse high-dimensional extremes allow for a parametric representation of the extremal dependence in order to handle it in a mathematically simpler way. **ExtremalDep** does the same thing, but also offers to model the extremal dependence in nonparametric and semiparametric ways, remaining more faithful to the nonparametric nature inherent to EVT. This manuscript illustrates the practical use of the package on important problems. In particular, it describes how to infer the extremal dependence in arbitrary dimension in a multivariate and spatial context, and how to use it to infer the probability of falling into a region considered extreme. Since the ordering between points is arbitrary in d -dimensional Euclidean spaces, definitions of useful concepts including extreme sets, multivariate extreme quantiles, quantile regions, joint tail and conditional probabilities and multivariate return levels are provided. In practice, these are used to: analyze the risk of urban cities being subject to future episodes of high pollution; identify regions of a country that are subject to high risk of heavy precipitations events; evaluate the risk of some regions being subject to future heat wave episodes, and so on.

The article is divided into two parts, Section 2 discusses multivariate extremes while Section 3 focuses on spatial extremes. In the multivariate part, Section 2.1 gives a brief introduction to the theoretical background while Section 2.3 details how to perform parametric (frequentist and Bayesian) inference for the extremal dependence in arbitrary dimension and for joint and conditional tail probabilities. Section 2.4 explains how to perform nonparametric Bayesian inference for the extremal dependence in arbitrary dimension and, once the extremal dependence has been estimated, how to infer joint and conditional tail probabilities in the bivariate case. The focus then successively shifts to the random generation of bivariate extreme values with a flexible semi-parametric dependence structure, the estimation of small probabilities of belonging to certain extreme sets and the estimation extreme quantile regions

corresponding to small joint tail probabilities.

2 Multivariate extremes

2.1 Background

Let $\mathbf{X}_1, \mathbf{X}_2, \dots$ be independent and identically distributed (i.i.d.) random vectors, where $\mathbf{X}_i = (X_{i,1}, \dots, X_{i,d}) \in \mathbb{R}^d$ with $d = 2, 3, \dots$, whose joint distribution F is in the domain of attraction of a multivariate *Generalised Extreme Value (GEV)* distribution G (de Haan and Ferreira, 2006, chap. 6), shortly denoted as $F \in \mathcal{D}(G)$. This implies that for $n = 1, 2, \dots$, there are norming sequences $\mathbf{a}_n > \mathbf{0} = (0, \dots, 0)$ and $\mathbf{b}_n \in \mathbb{R}^d$ such that

$$\lim_{n \rightarrow \infty} F^n(\mathbf{a}_n \mathbf{x} + \mathbf{b}_n) = G_\gamma(\mathbf{x} | D), \quad \mathbf{x} \in \mathbb{R}^d, \quad (2.1)$$

where $\gamma = (\gamma_1, \dots, \gamma_d)^\top \in \mathbb{R}^d$. The limiting distribution can be written as

$$G_\gamma(\mathbf{x} | D) = C_{\text{EV}}(G_{\gamma_1}(x_1), \dots, G_{\gamma_d}(x_d) | D), \quad \mathbf{x} \in \mathbb{R}^d, \quad (2.2)$$

where C_{EV} is an *extreme-value copula* (Beirlant et al., 2004, chap. 8) and for all $j \in \{1, \dots, d\}$ the marginal distributions are of the form

$$G_{\gamma_j}(x_j) = \exp\left(- (1 + \gamma_j x_j)^{-\frac{1}{\gamma_j}}\right), \quad 1 + \gamma_j x_j > 0, \quad (2.3)$$

i.e., univariate GEV distributions with *extreme value index* $\gamma_j \in \mathbb{R}$ describing the tail heaviness of the distribution (e.g., de Haan and Ferreira, 2006, chap. 1). In particular, the extreme-value copula takes the form

$$C_{\text{EV}}(\mathbf{u} | D) = \exp(-L((-\ln u_1), \dots, (-\ln u_d))), \quad \mathbf{u} \in (0, 1]^d, \quad (2.4)$$

where $L : [0, \infty)^d \mapsto [0, \infty)$ is a homogeneous function of order 1 named *stable-tail* dependence function (Beirlant et al., 2004, chap. 8). This function is fully characterised by its restriction on $\mathcal{R} := \{\mathbf{t} \in [0, 1]^{d-1} : \|\mathbf{t}\|_1 \leq 1\}$ which is known as the Pickands dependence function (e.g., Falk et al., 2010, Ch. 4) and defined as

$$A(\mathbf{t}) = L(1 - t_1 - \dots - t_{d-1}, \mathbf{t}) = d \int_{\mathcal{S}} \max\{(1 - t_1 - \dots - t_{d-1})w_1, \dots, t_{d-1}w_d\} dH(\mathbf{w}), \quad (2.5)$$

where H is a probability measure on the d -dimensional unit simplex $\mathcal{S} := \{\mathbf{w} \geq \mathbf{0} : \|\mathbf{w}\|_1 = 1\}$, named *angular measure* (e.g., Falk et al., 2010, Ch. 4). A valid angular measure is a probability measure that satisfies the mean constraint (C1), while a valid Pickands dependence function is a function that must satisfy the convexity and boundary conditions (C2)-(C3). Specifically,

$$(C1) \int_{\mathcal{S}} w_j H(d\mathbf{w}) = 1/d, \quad \forall j \in \{1, \dots, d\}.$$

$$(C2) A(a\mathbf{t}_1 + (1-a)\mathbf{t}_2) \leq aA(\mathbf{t}_1) + (1-a)A(\mathbf{t}_2), \quad a \in [0, 1], \quad \forall \mathbf{t}_1, \mathbf{t}_2 \in \mathcal{R},$$

$$(C3) 1/d \leq \max(t_1, \dots, t_{d-1}, 1 - t_1 - \dots - t_{d-1}) \leq A(\mathbf{t}) \leq 1, \quad \forall \mathbf{t} \in \mathcal{R}.$$

Conditions (C2)-(C3) are necessary and sufficient to define a valid Pickands dependence function only in the bivariate case, (for details see [Beirlant et al., 2004](#), chap. 8). Since A and H are related through the one-to-one map in (2.5), the dependence parameter D of the copula $C_{\text{EV}}(\cdot | D)$ is commonly meant to be either the angular measure or the Pickands dependence function. Both are possible means to describe the so-called *extremal dependence*.

Given a sample $(\mathbf{X}_1, \dots, \mathbf{X}_N)$ with joint distribution $F \in \mathcal{D}(G)$, for each margin $j \in \{1, \dots, d\}$, k maxima are computed over blocks of size n , such that $N = n \cdot k$, where the i th maximum given by $M_{i,j}^{(n)} = \max(X_{(i-1)n+1,j}, \dots, X_{in,j})$, $i \in \{1, \dots, k\}$. The vector of componentwise maxima is then defined as $\mathbf{M}_{n,i} = (M_{i,j}^{(n)}, 1 \leq j \leq d)$. Setting $\boldsymbol{\mu} = \mathbf{b}_n$, $\boldsymbol{\sigma} = \mathbf{a}_n$, $\mathbf{y} = \mathbf{a}_n \mathbf{x} + \mathbf{b}_n$, by (2.1), the joint distribution of $\mathbf{M}_{n,i}$ can be approximated, for large enough n , as $F^n(\mathbf{y}) \approx G_{\boldsymbol{\theta}}(\mathbf{y} | D)$, where $\boldsymbol{\theta} = (\boldsymbol{\mu}, \boldsymbol{\sigma}, \boldsymbol{\gamma})^\top$ and each one-dimensional marginal distribution regarding the maximum $M_{i,j}^{(n)}$ can be approximated as

$$F^n(y_j) \approx G_{\theta_j}(y_j) = \exp \left(- \left(1 + \gamma_j \frac{y_j - \mu_j}{\sigma_j} \right)^{-\frac{1}{\gamma_j}} \right), \quad j \in \{1, \dots, d\}. \quad (2.6)$$

The dependence among the maxima $(M_{i,1}^{(n)}, \dots, M_{i,d}^{(n)})$ can be approximated by the extreme-value copula $C_{\text{EV}}(\cdot | D)$, where if the parameter D is the angular measure H , it describes the dependence among maxima as follows: the more mass H places around the centre of the simplex $(1/d, \dots, 1/d)$ the more dependent the maxima are. Conversely, the maxima becomes less dependent as H concentrates its mass close to the vertices of the simplex. Alternatively, D can be the Pickands dependence function with the lower and upper bounds in the inequality in (C3) respectively representing the cases of complete dependence and independence. A useful summary of the dependence among the maxima is given by the so-called *extremal coefficient* (e.g., [Beirlant et al., 2004](#), Ch. 8), defined as

$$\eta = dA(1/d, \dots, 1/d), \quad (2.7)$$

which represents the (fractional) number of independent block maxima. The extremal coefficient satisfies $1 \leq \eta \leq d$, with the lower and upper bounds describing the case of complete dependence and independence.

Beyond these results, the domain of attraction provides also a useful basis to derive very small joint tail probabilities corresponding to high-dimensional extremes relative to the original distribution F or to derive extreme quantile regions corresponding to very small joint tail probabilities. These results are summarized as follows. The limit in (2.1) holds if and only if $n(1 - F(\mathbf{a}_n \mathbf{x} + \mathbf{b}_n)) \rightarrow -\log G(\mathbf{x})$ as $n \rightarrow \infty$, for all $\mathbf{x} \in \mathbb{R}^d$, with the convention that $-\log(0) = \infty$. Together with the weak convergence of the copula of the vector of componentwise maxima, namely $\{C(\mathbf{u}^{1/n})\}^n \rightarrow C_{\text{EV}}(\mathbf{u})$ as $n \rightarrow \infty$, for all $\mathbf{u} \in (0, 1]^d$, this result implies that for all $\mathbf{x} \in [0, \infty)^d$, as $n \rightarrow \infty$,

$$n \mathbb{P} \left(\bigcup_{j=1}^d F_j(X_j) > 1 - \frac{x_j}{n} \right) \rightarrow L(\mathbf{x}) = d \int_{\mathcal{S}} \max_{j=1, \dots, d} (x_j w_j) dH(\mathbf{w}).$$

Recall that a copula C defined on $[0, 1]^d$ and associated to a joint distribution function F , is a suitable function that allows the definition $F(\mathbf{x}) = C(F_1(x_1), \dots, F_d(x_d))$ (see e.g., [Joe, 2014](#), for details). For simplicity we assume that the margins of F are continuous. The result

in the above display implies the following important approximation. Let $p_j = p_{n,j} = x_j/n$ for $j = 1, \dots, d$ and $Q_j(p_j)$ be the $(1-p)$ -quantile of F_j , then by homogeneity of the stable tail dependence function, the probability that at least one among the d variables X_j exceeds a high quantile of its own distribution, can be approximated for large n as

$$\mathbb{P}(X_1 > Q_1(p_1) \text{ or } \dots \text{ or } X_d > Q_d(p_d)) \approx L(p_1, \dots, p_d). \quad (2.8)$$

By the inclusion and exclusion principle, the weak convergence result of the extreme value copula also allows to obtain

$$n \mathbb{P} \left(\bigcap_{j=1}^d F_j(X_j) > 1 - \frac{x_j}{n} \right) \rightarrow R(\mathbf{x}) = d \int_{\mathcal{S}} \min_{j=1, \dots, d} (x_j w_j) dH(\mathbf{w}), \quad n \rightarrow \infty,$$

where R is known as the *tail copula* function, which is also a homogeneous function of order 1, and therefore the probability that all the d variables (X_1, \dots, X_d) exceed simultaneously high quantiles of their own distributions can be approximated, for a sufficiently large n , as

$$\mathbb{P}(X_1 > Q_1(p_1) \text{ and } \dots \text{ and } X_d > Q_d(p_d)) \approx R(p_1, \dots, p_d). \quad (2.9)$$

Finally, a related question is, how to determine an extreme region given a small joint probability p of falling in it? The approach discussed by [Cai et al. \(2011\)](#), [Einmahl et al. \(2013\)](#) and [He and Einmahl \(2017\)](#) is summarized as follows with a focus on the bivariate case explored by [Einmahl et al. \(2013\)](#). Let f be the density on \mathbb{R}_+^2 of a bivariate distribution F satisfying $F \in \mathcal{D}(G)$, with $\gamma_1, \gamma_2 > 0$. Define quantile regions by the level sets of f such that

$$\mathcal{Q} = \{\mathbf{x} \in \mathbb{R}_+^2 : f(\mathbf{x}) \leq \alpha\}, \quad (2.10)$$

with $\alpha > 0$. Then, for a small probability $p > 0$ we derive the region \mathcal{Q} such that $\mathbb{P}(\mathcal{Q}) = p$ and f everywhere on \mathcal{Q} is smaller than f everywhere on \mathcal{Q}^c and therefore the latter is the smallest region satisfying $\mathbb{P}(\mathcal{Q}^c) = 1 - p$. Accordingly, an *extreme quantile region* is defined by a level set \mathcal{Q}_N (with $\alpha = \alpha_N$ in (2.10)), which is such that $\mathbb{P}(\mathcal{Q}_N) = p$ where $p = p_N \rightarrow 0$ and the expected number of points falling in it is $Np \rightarrow c > 0$ as $N \rightarrow \infty$. Note that when $c < 1$, the region is so extreme that almost no observations are expected to fall in it.

The domain of attraction condition implies the existence of a measure ξ , named *exponent measure*, such that

$$N \mathbb{P}(\{Q_1(1/N)x_1^{\gamma_1}, Q_2(1/N)x_2^{\gamma_2} : \mathbf{x} \in B\}) \rightarrow \xi(B), \quad N \rightarrow \infty$$

and satisfying $\xi(\partial B) = 0$, for all Borel set $B \subset [0, \infty]^2$ that are bounded away from the origin. Assume that f is bounded away from zero on $(0, M]^2$ and, outside this region, f is decreasing in each coordinate, for some $M > 0$. Assume also that the exponent measure admits a density function g such that

$$\xi(\{\mathbf{v} : v_1 > x_1 \text{ or } v_2 > x_2\}) = \int \int_{\{v_1 > x_1 \text{ or } v_2 > x_2\}} g(\mathbf{v}) d\mathbf{v},$$

and

$$N Q_1(1/N) Q_2(1/N) f(Q_1(1/N)x_1^{\gamma_1}, Q_2(1/N)x_2^{\gamma_2}) \rightarrow \frac{x_1^{1-\gamma_1} x_2^{1-\gamma_2}}{\gamma_1 \gamma_2} g(\mathbf{x}) =: q(\mathbf{x}), \quad N \rightarrow \infty.$$

In particular, we have that g is related to the density h of the angular measure H by $h(w) = 2^{-1}g(w, 1-w)$, where $w = x_1/r$ and $r = x_1 + x_2$. The basic set S is defined as $S = \{\mathbf{x} : q(\mathbf{x}) \leq 1\} = \{\mathbf{x} : r \geq q_\star^{-1}(w), w \in [0, 1]\}$, where

$$q_\star(w) = \left(2\gamma_1^{-1}\gamma_2^{-1}w^{1-\gamma_1}(1-w)^{1-\gamma_2}h(w)\right)^{-\frac{1}{1+\gamma_1+\gamma_2}},$$

and, according to the exponent measure, its size is equal to

$$\xi(S) = 2 \int_{[0,1]} q_\star(w)h(w)dw.$$

The set S is then suitably transformed in order to obtain for \mathcal{Q}_N the approximation

$$\tilde{\mathcal{Q}}_N = \left\{ \left(\mu_1 + \sigma_1 \frac{\left(\frac{k\xi(S)x_1}{Np}\right)^{\gamma_1} - 1}{\gamma_1}, \mu_2 + \sigma_2 \frac{\left(\frac{k\xi(S)x_2}{Np}\right)^{\gamma_2} - 1}{\gamma_2} \right) : \mathbf{x} \in S \right\}, \quad (2.11)$$

where $k = k_N$ with $k \rightarrow \infty$ as $N \rightarrow \infty$ and $k = o(N)$. Furthermore, $\mu_j = Q_j(k/N)$ and $\sigma_j = a_j(N/k)$ with $j = 1, 2$, where $a_j(\cdot)$ is a suitable positive scale function (de Haan and Ferreira, 2006, Ch. 1-2). $\tilde{\mathcal{Q}}_N$ is a good approximation of \mathcal{Q}_N in the sense that $\mathbb{P}(\tilde{\mathcal{Q}}_N) \approx p$ and $\mathbb{P}(\mathcal{Q}_N \Delta \tilde{\mathcal{Q}}_N) \rightarrow 0$ as $N \rightarrow \infty$ (see Einmahl et al., 2013), where $A \Delta B = A \setminus B \cup B \setminus A$.

2.2 Statistical challenges

From a statistical perspective, the multivariate GEV model defines a complex semiparametric family of distributions of the form $G_\theta(\mathbf{y} | D) = C_{\text{EV}}(G_{\theta_1}(y_1), \dots, G_{\theta_d}(y_d) | D)$, $\mathbf{y} \in \mathbb{R}^d$, where $\theta \in \Theta \subset (\mathbb{R}, \mathbb{R}_+, \mathbb{R})^d$ is a finite-dimensional vector of marginal parameters and D is an infinite-dimensional dependence parameter of the copula C_{EV} , named extremal dependence, living in a suitable space, depending whether D is the angular measure or the Pickands dependence function. The estimation of such infinite-dimensional parameter, accounting for the corresponding constraints (see conditions (C1)-(C3) of Section 2.1), is far from being a simple task. To reduce complexity, classes of parametric models were initially proposed to model D , see Beranger and Padoan (2015) for a review. In order to provide valid extremal dependence structures, the proposed models satisfy the required constraints. Section 2.3 describes how to fit some of the most popular parametric models for D using **ExtremalDep**.

Over time, more sophisticated semi- and non-parametric approaches for modelling and estimating the extremal dependence have been proposed, under both parametrisations. Some examples include: projection estimators (e.g., Fils-Villetard et al., 2008), polynomials (e.g., Marcon et al., 2017) and splines (e.g., Cormier et al., 2014), just to name a few. Section 2.4 details how to use **ExtremalDep** for non-parametric estimation of the extremal dependence, simulation of bivariate extreme values with a flexible semi-parametric dependence structure, estimation of small probabilities to belong to certain extreme sets and estimation extreme quantile regions corresponding to small joint tail probabilities.

2.3 Parametric modelling of the extremal dependence

A non-exhaustive list of popular parametric models for the extremal dependence includes the Asymmetric-Logistic, Pairwise-Beta, Tilted-Dirichlet, Hüsler-Reiss, Extremal- t and Extremal-Skew- t models (see e.g., Beranger and Padoan, 2015; Beranger et al., 2017).

The Poisson-Point-Process (PPP) is a simple estimation method for statistical models used to represent the extremal dependence, when the latter is parametrized according to the angular measure and provided that it allows for a density $h(w|\varphi)$ on \mathcal{S} , where φ is a suitable vector of parameters (see e.g., [Coles and Tawn, 1991](#); [Engelke et al., 2015](#)). In particular, let $\mathbf{x}_1, \dots, \mathbf{x}_N$ be i.i.d. observations from $F \in \mathcal{D}(G)$ and $\mathbf{y}_1, \dots, \mathbf{y}_N$ be their equivalent with unit Fréchet margins. The pseudopolar transformation T is defined as $T(\mathbf{y}_i) = (r, \mathbf{w}_i)$ where $r = \mathbf{y}_1 + \dots + \mathbf{y}_N$ is the radial part and $\mathbf{w}_i = \mathbf{y}_i/r$ is the angular part of \mathbf{y}_i , $i = 1, \dots, N$. The domain of attraction condition implies that if r_0 is a large threshold and $W_{r_0} = \{(r, \mathbf{w}) : r > r_0\}$ is a set of points with a radial component larger than r_0 , then the number of points falling in W_{r_0} is described approximatively by a Poisson random variable with rate $1/\psi(W_{r_0})$, where $\psi = \xi(T^{-1}(\cdot))$. Thus, conditionally on observing k points $\{(r_{(i)}, \mathbf{w}_{(i)}), i = 1, \dots, k\}$ with radial part greater than r_0 , such points are approximately independent and generated from the density function $(r^{-2}dr \times H(d\mathbf{w}))/\psi(W_{r_0})$. The likelihood function of the exceedances can then be approximated as

$$L(\varphi \mid (r_{(i)}, \mathbf{w}_{(i)}), i = 1, \dots, k) \approx \frac{e^{-\psi(W_{r_0})}(\psi(W_{r_0}))^k}{k!} \prod_{i=1}^k \frac{r_{(i)}^{-2} h(\mathbf{w}_{(i)} \mid \varphi)}{\psi(W_{r_0})} \\ \propto h(\mathbf{w}_{(i)} \mid \varphi).$$

Estimates of φ can be obtained by maximizing the log-likelihood $\ell(\varphi) = \sum_{i=1}^k \log h(\mathbf{w}_{(i)} \mid \varphi)$. Alternatively, one can appeal to a Bayesian approach ([Sabourin et al., 2013](#)), based on the approximate posterior density of the angular density parameters given by

$$\pi(\varphi \mid \mathbf{w}_{(1)}, \dots, \mathbf{w}_{(k)}) = \frac{\prod_{i=1}^k h(\mathbf{w}_{(i)} \mid \varphi) \phi(\varphi)}{\int_{\Psi} \prod_{i=1}^k h(\mathbf{w}_{(i)} \mid \varphi) \phi(\varphi) d\varphi},$$

where $\phi(\varphi)$ is a suitable prior distribution on φ and Ψ is a suitable parameter space.

The routine `fExtDep` with argument `method="PPP"` allows to estimate φ by likelihood maximisation. The model class for h is specified with the argument `model` with the list of available options reported in [Table 2](#). Some classes of models are characterised by an angular density $h(\mathbf{w} \mid \varphi)$ that places a continuous mass only in the interior of \mathcal{S} (PB, TD, HR), while others also allow to place densities and atoms on subspaces of \mathcal{S} . [Beranger et al. \(2017\)](#) describe an extended version of the ML method that allows for the estimation of these more complex models up to the three-dimensional case (AL, ET, EST) by exploiting the following approach. In the bivariate case, an observation $\mathbf{w} = (w, 1 - w)$ falls at an endpoint of \mathcal{S} if $w < c$ or $w > 1 - c$ for some small $c \in (0, 1/2)$ and on the interior of \mathcal{S} otherwise. A trivariate observation $\mathbf{w} = (w_1, w_2, 1 - w_1 - w_2)$ falls: at the j th corner of \mathcal{S} if $\mathbf{w} \in \mathcal{C}_j = \{w_j > 1 - c\}$, on the edge between the j th and l th components if $\mathbf{w} \in \mathcal{E}_{j,l} = \{w_j, w_l < 1 - c, w_j + w_l > 1 - c, w_j > 1 - 2w_l, w_l > 1 - 2w_j\}$, and in the interior of \mathcal{S} otherwise (i.e., if $w_j > c$, for all j) (see [Beranger et al., 2017](#), for details). This approach is implemented when specifying a positive value for the argument `c` of `fExtDep`.

We now illustrate the use of `fExtDep` on the analysis of high levels of air pollution recorded in Leeds, UK, over the winter period November 1st to February 27/28th, between 1994 and 1998 (see [Heffernan and Tawn, 2004](#)). The object `pollution` contains the daily maximum of the five air pollutants: particulate matter (PM10), nitrogen oxide (NO), nitrogen dioxide (NO2), ozone (O3), and sulfur dioxide (SO2), in unit Fréchet scale (for a description on the used transformation see [Beranger and Padoan, 2015](#)). Furthermore, the datasets PNS, NSN

and PNN contains the angular components corresponding to the 100 largest radial components of the triplets of pollutants (PM10, NO, SO2), (NO2, SO2, NO) and (PM10, NO, NO2), respectively. We run the following simple commands

```
R> data(pollution)
R> f.et05 <- fExtDep(method="PPP", data=PNS, model = "ET",
+                   par.start = c(0.5, 0.5, 0.5, 3), trace=2, c=0.05)

initial value -118.269640
iter 10 value -146.907539
iter 10 value -146.907539
final value -146.907539
converged

R> f.et <- fExtDep(method="PPP", data=PNS, model = "ET",
+                 par.start = c(0.5, 0.5, 0.5, 3), trace=2 )

initial value -161.078869
iter 10 value -225.654851
iter 20 value -234.524086
iter 30 value -235.285461
iter 40 value -235.360084
final value -235.382293
converged
```

The first call to the `fExtDep` routine fits the Extremal- t angular density (`model="ET"`), to the pollution data (`data=PNS`), allowing for point masses at the corners by specifying the argument `c`, while the second call considers a density defined only in the interior of \mathcal{S} . The argument `par.start` gives starting values for the parameters and `trace=2` allows to monitor optimization progress. The optimization method is set by the argument `optim.method` ("BFGS" by default) on which basis the routine `optim` from the `stats` library is used. `fExtDep` returns a list with the estimates of the model parameters (`par`), their standard errors (SE), the log-likelihood maximum (LL) and the Takeuchi Information Criterion (TIC). `fExtDep` is first ran for the extremal- t model using different values of c (0, 0.05 and 0.1) to take into account point masses at the corners of \mathcal{S} . The TICs indicate that only assuming mass in the interior of \mathcal{S} provides the best results (lowest TIC). A performance comparison between the PB, AL, TD, HR, ET and EST models defined on the interior only, is performed with TIC scores reported in Table 1 and as a result the Extremal skew- t model fits the data best (lowest TIC).

model	PB	AL	TD	HR	ET	EST
TIC	-188.75	-406.85	-393.75	-460.25	-461.74	-493.31

Table 1: TIC of models fitted to PNS data obtained using `fExtDep` with $c=0$.

Bayesian inference for the parameter φ is implemented through a model averaging approach (Sabourin et al., 2013) and available in the routine `fExtDep` when `method="BayesianPPP"`. Table 2 reports the implemented prior densities for each angular density model. In particular,

$\phi(\cdot, a, b)$ stands for a one-dimensional Gaussian density with mean a and variance b , $t(\cdot)$ is a transformation applied to the parameter (to map it to the real line). For each component of φ , the proposal density is also Gaussian but of the form $\phi(t(\varphi_j^*); t(\varphi_j^{(i)}), \text{MCpar})$, where φ_j^* and $\varphi_j^{(i)}$ are the proposed value and the value at the i th iteration of the algorithm of the j element of φ , respectively, and MCpar is the variance term that needs to be specified by the user. The next display illustrates how to perform Bayesian inference for the Hüsler-Reiss model (`model="HR"`) considering `Nsim=5e+4` iterations, a burn-in period of `Nbin=3e+4` iterations, hyper-parameters `Hpar=Hpar.hr`, `MCpar=0.35` and using the argument `seed` for reproducibility. Refer to the help page for a description of the list returned as output from `fExtDep`.

```
R> Hpar.hr <- list(mean.lambda=0, sd.lambda=3)
R> PNS.hr <- fExtDep(method="BayesianPPP", data=PNS, model="HR", Nsim=5e+4,
+                   Nbin=3e+4, Hpar=Hpar.pb, MCpar=0.35, seed=14342)

|=====| 100%

R> labs <- c(expression(PM[10]), expression(NO), expression(SO[2]))
R> plot.ExtDep(object="angular", model="HR", par=PNS.hr$emp.mean,
+             data=PNS, cex.lab=2, labels=labs)
```

The empirical mean (standard deviation) obtained from the approximate posterior distribution of $(\hat{\lambda}_{1,2}, \hat{\lambda}_{1,3}, \hat{\lambda}_{2,3})$ are $(0.65(0.04), 0.90(0.04), 0.98(0.04))$, while the Bayesian Information Criterion (BIC) is -449.64 . Visualisation of the fitted angular density is obtained from the routine `plot.ExtDep` by specifying `object = "angular"` and `model="PB"`, and selecting the parameters to be the mean of the approximate posterior distribution (`par=fit.hr$emp.mean`). The argument `data = PNS` plots the angular data on top of the estimated density. Figure 1 showcases a dependence structure that appears to follow the data structure well but other models should be fitted (see [Beranger and Padoan, 2015](#), for further details).

Model	model	φ	$t(\cdot)$	Prior
Pairwise-Beta	PB	$(\alpha, \beta_{i,j})$	log	$\phi(\log(\alpha); \text{mean.alpha}, \text{sd.alpha})$
			log	$\phi(\log(\beta_{i,j}); \text{mean.beta}, \text{sd.beta})$
Asymmetric-Logistic	AL	$(\alpha_S, \beta_{j,S})$	log	$\phi(\log(\alpha_S); \text{mean.alpha}, \text{sd.alpha})$
			logit	$\phi(\text{logit}(\beta_{j,S}); \text{mean.beta}, \text{sd.beta})$
Tilted-Dirichlet	TD	α_j	log	$\phi(\log(\alpha_j); \text{mean.alpha}, \text{sd.alpha})$
Hüsler-Reiss	HR	$\lambda_{i,j}$	log	$\phi(\log(\lambda_{i,j}); \text{mean.lambda}, \text{sd.lambda})$
Extremal- t	ET	$(\rho_{i,j}, \nu)$	atanh	$\phi(\text{atanh}(\rho_{i,j}); \text{mean.rho}, \text{sd.rho})$
			log	$\phi(\log(\nu); \text{mean.nu}, \text{sd.nu})$
Extremal-Skew- t	EST	$(\rho_{i,j}, \alpha_i, \nu)$	atanh	$\phi(\text{atanh}(\rho_{i,j}); \text{mean.rho}, \text{sd.rho})$
			identity	$\phi(\alpha_i; \text{mean.alpha}, \text{sd.alpha})$
			log	$\phi(\log(\nu); \text{mean.nu}, \text{sd.nu})$

Table 2: List of available angular density model families and prior densities that are considered with them when using `fExtDep(method="BayesianPPP", ...)`.

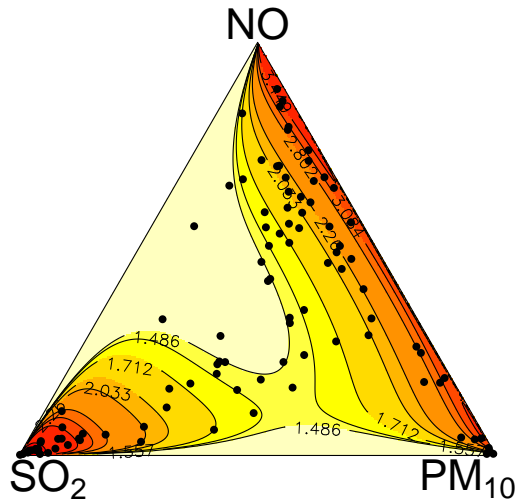


Figure 1: Estimated angular densities from the Hüsler-Reiss model.

The purpose of estimating the extremal dependence is to estimate small tail probabilities as in (2.9). Similar to Cooley et al. (2010), we define the extreme event $\{\text{PM}_{10} > 95, \text{NO} > 270, \text{SO}_2 > 95\}$ and infer this probability using the routine `pExtDep` with `method="Parametric"`, `type="upper"` and specifying the argument `model`. Providing a vector to `par` yields a point estimate of the tail probabilities while a matrix (e.g., the posterior sample) with rows of parameter values derives an approximate posterior distribution for such probabilities. Note that the object `est` and the routine `transform` are used to transform values to unit Fréchet scale following the steps of Heffernan and Tawn (2004).

```
R> est.fun <- function(x){
+   x <- na.omit(x)
+   unlist(evd::fpot(x, threshold=quantile(x, probs=0.7))
+         [c("threshold", "estimate")])
+ }

R> est <- apply(winterdat, 2, est.fun)

R> transform <- function(x, data, par){
+   data <- na.omit(data)
+   if(x > par[1]){
+     emp.dist <- mean(data <= par[1])
+     dist <- 1-(1-emp.dist)*max(0, 1+par[3]*(x-par[1])/par[2])^(-1/par[3])
+   }else{
+     dist <- mean(data <= x)
+   }
+   return(-1/log(dist))
+ }

R> th <- c(95, 270, 110, NA, 95)
```

```

R> Th <- sapply(c(1:3,5), function(x) transform(th[x], data=winterdat[,x], par=est[,x]) )
R> names(Th) <- colnames(winterdat[c(1:3,5)])
R> xl.PNS <- bquote("P(" * PM[10] ~ ">" ~ .(th[1]) * ", NO" ~ ">" ~ .(th[2])
+
* ", " * SO[2] ~ ">" ~ .(th[5]) * ")")
R> P.PNS <- pExtDep(q=Th[colnames(PNS)], type="upper", method="Parametric",
+
model="HR", par=PNS.hr$stored.vals, xlab=xl.PNS)

```

The left panel of Figure 2 provides the approximate posterior distribution of the tail probabilities in (2.9) for the extreme events. Note that a smoother output could be obtained by considering $N_{\text{sim}}=5e+5$ and $N_{\text{burn}}=3e+5$. Formula (2.9) can also be used to derive a possible definition of the so-called *joint return level*, see Beranger and Padoan (2015) for details, i.e. the sequence of values $y_{j;p}, j \in J \subset \{1, \dots, d\}$, that satisfies the equation

$$p = \mathbb{P}(Y_j > y_{j;p}, X_i > x_i, j \in J, i \in \{1, \dots, d\}nJ),$$

for a given small probability $p \in (0, 1)$, where x_i , with $i \in \{1, \dots, d\}nJ$ is a sequence of fixed high thresholds. Below is an example where the routine `plot_ExtDep` is used to infer joint return levels. Here only a subset of the posterior is considered for a quick evaluation but in practice, we do recommend using the full posterior.

```

R> Q.fix <- c(NA, Th[c(2,4)])
R> PM10.range <- seq(from=est[1,1], to=400, by=5)
R> Q.range <- sapply(PM10.range, transform, data=winterdat[,1], par=est[,1])
R> set.seed(1)
R> ind <- sample(1:2e+4, 100)
R> rl.PM10 <- plot_ExtDep(object="returns", model="HR",
+
par=PNS.hr$stored.vals[ind,], Q.fix=Q.fix,
+
Q.range=Q.range, Q.range0=PM10.range,
+
labels=expression(PM[10]), main=bquote("Return level
+
for" ~ PM[10] ~ "when NO" ~ ">" ~ .(th[2]) ~ "and" ~
+
SO[2] ~ ">" ~ .(th[5]) ), cex.lab=1.4, cex.axis=1.4)

```

Returns levels are displayed when `object="returns"`. In addition, it requires to provide `Q.fix`, a vector of length equal to the model dimension (2 or 3), where quantile values can be fixed for some components while others (NAs) are left to vary. The `Q.range` argument provides a vector (or matrix) of quantile values on the unit Fréchet scale, for those that aren't fixed. If `Q.fix` contains a single NA then `Q.range` must be a vector or a single column matrix. `Q.range0` provide the same sequences as `Q.range` but on the original scale. This plotting procedure relies on the `pExtDep` routine. The middle panel of Figure 2 reports the univariate joint return level curve for PM_{10} jointly to the extreme event $\{NO > 270, SO_2 > 95\}$, corresponding to the return period $1/p$, which has been estimated by the approximate posterior mean and uncertainty is given by the 95% (pointwise) credibility intervals. Similarly, the right panel of Figure 2 depicts the posterior mean and 95% credibility intervals of the estimated contour levels of the bivariate return levels for (PM_{10}, NO) jointly to extreme event $SO_2 > 95$. Note that conditional return levels can be obtained by specifying `cond=TRUE`, the conditional event being the fixed event.

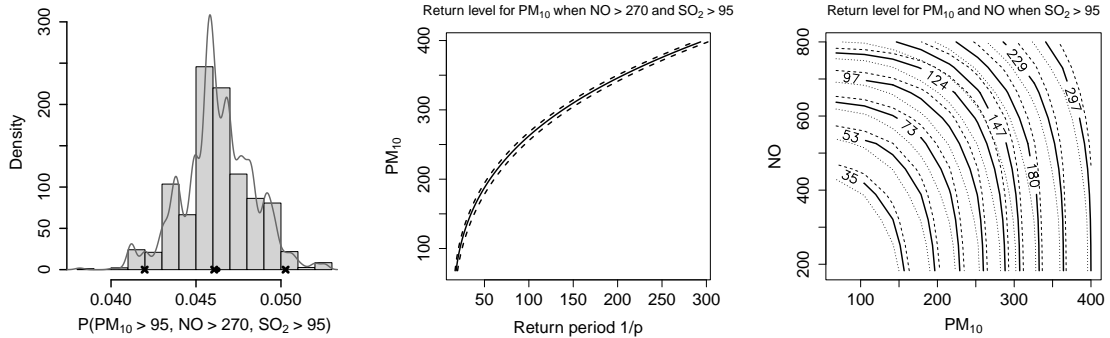


Figure 2: Left panel shows the approximate posterior distribution of tail probability with crosses indicating posterior median and 95% (pointwise) credibility interval and a dot indicating the posterior mean. Middle and right panels show the posterior mean (solid line) and posterior 95% credibility interval (dashed lines) of univariate and bivariate return levels associated with return period $1/p$, when respectively fixing two and one components.

2.4 Semi- and non-parametric modeling of the extremal dependence

Common objectives when analyzing extreme values include assessment of the dependence level among extremes, e.g. using the dependence structures in (2.4)-(2.5), simulation of multiple extremes, estimation of small joint tail probability, e.g. (2.8)-(2.9), and estimation of extreme quantile regions. The next sections describe the steps required to accomplish such goals.

2.4.1 Extremal dependence estimation via Bernstein polynomials

Below, we give a brief summary of a simple estimation method for the extremal dependence with an arbitrary number of componentwise maxima proposed by Marcon et al. (2017). We refer to the aforementioned paper for further details.

The method consists of two steps: 1) a nonparametric pilot estimation of the Pickands dependence function, 2) a regularization of such estimate by projecting it into a polynomial representation in Bernstein form imposing conditions (C2)-(C3). Given some i.i.d. random vectors $\mathbf{Y}_1, \dots, \mathbf{Y}_k$ (approximately) distributed as the multivariate GEV distribution in (2.2), the first step is achieved by using the madogram-based estimator of the Pickands dependence function. This is given, for all $\mathbf{t} \in \mathcal{R}$, by

$$\hat{A}_k(\mathbf{t}) = \frac{\hat{\nu}_k(\mathbf{t}) + d^{-1} \sum_{j=1}^d (t_j / (1 + t_j))}{1 - \hat{\nu}_k(\mathbf{t}) - d^{-1} \sum_{j=1}^d (t_j / (1 + t_j))},$$

where

$$\hat{\nu}_k(\mathbf{t}) = \frac{1}{k} \sum_{i=1}^k \left(\max_{1 \leq j \leq d} F_{k,j}^{1/t_j}(Y_{i,j}) - \frac{1}{d} \sum_{j=1}^d F_{k,j}^{1/t_j}(Y_{i,j}) \right),$$

and $F_{k,j}$ denotes the empirical distribution of the j th variable. For the regularization of the pilot estimate, take $\kappa > d$ and let Γ_κ be the set of multi-indices $\boldsymbol{\alpha} = (\alpha_1, \dots, \alpha_d) \in \{0, 1, \dots, \kappa\}^d$ such that $\alpha_1 + \dots + \alpha_d = \kappa$ and $\alpha_d = \kappa - \alpha_1 - \dots - \alpha_{d-1}$, whose cardinality is denoted by $C_\kappa = |\Gamma_\kappa|$. Let

$$A_\kappa(\mathbf{t}) = \sum_{\boldsymbol{\alpha} \in \Gamma_\kappa} \beta_{\boldsymbol{\alpha}} b_{\boldsymbol{\alpha}}(\mathbf{t}, \kappa), \quad \mathbf{t} \in \mathcal{R}, \quad (2.12)$$

be the Bernstein-Bézier polynomial representation of the Pickands dependence function, where for each $\alpha \in \Gamma_\kappa$,

$$b_\alpha(\mathbf{t}, \kappa) = \frac{\kappa!}{\prod_{j=1}^d \alpha_j!} \prod_{j=1}^{d-1} t_j^{\alpha_j} (1 - t_1 - \dots - t_{d-1})^{\alpha_d}, \quad \mathbf{t} \in \mathcal{R}, \quad (2.13)$$

is the Bernstein polynomial basis function of index α and degree κ .

Now, let \mathcal{A} be the family of functions $f : \mathcal{R} \rightarrow [1/d, 1]$ satisfying conditions (C2)-(C3), and $\mathcal{A}_\kappa = \{\mathbf{t} \mapsto \mathbf{b}_\kappa(\mathbf{t})\boldsymbol{\beta}_\kappa; \boldsymbol{\beta}_\kappa \in [0, 1]^{p_\kappa} \text{ such that } \mathbf{R}_\kappa \boldsymbol{\beta}_\kappa \geq \mathbf{r}_\kappa\}$ be a sequence of families of constrained multivariate Bernstein-Bézier polynomials on \mathcal{R} , where $\mathbf{b}_\kappa(\mathbf{t})$ is the row vector $(b_\alpha(\mathbf{t}, \kappa), \forall \alpha \in \Gamma_\kappa)$, $\boldsymbol{\beta}_\kappa$ is a column vector, \mathbf{R}_κ is a suitable $(q \times p_\kappa)$ matrix of full row rank and \mathbf{r}_κ is a $(q \times 1)$ vector. The constraint $\mathbf{R}_\kappa \boldsymbol{\beta}_\kappa \geq \mathbf{r}_\kappa$ on the coefficient vector $\boldsymbol{\beta}_\kappa$ guarantees that each member of \mathcal{A}_κ satisfies (C2)-(C3). A projection estimator of the Pickands dependence function based on the estimator $\hat{A}_k(\mathbf{t})$ is the solution to the following optimization problem

$$\tilde{A}_{k,\kappa} = \arg \min_{f \in \mathcal{A}_\kappa} \|\hat{A}_k - f\|.$$

For a finite set of points $\{\mathbf{t}_u : u = 1, \dots, U\}$, with $U = 1, 2, \dots$ and $\mathbf{t}_u \in \mathcal{R}$ such a solution is obtained by finding the minimizer $\hat{\boldsymbol{\beta}}_\kappa$ of the constrained least-squares problem

$$\hat{\boldsymbol{\beta}}_\kappa = \arg \min_{\boldsymbol{\beta}_\kappa \in [0, 1]^{p_\kappa} : \mathbf{R}_\kappa \boldsymbol{\beta}_\kappa \geq \mathbf{r}_\kappa} \frac{1}{U} \sum_{u=1}^U (\mathbf{b}_\kappa(\mathbf{t}_u) \boldsymbol{\beta}_\kappa - \hat{A}_k(\mathbf{t}_u))^2,$$

which expression is

$$\hat{\boldsymbol{\beta}}_\kappa = (\mathbf{b}_\kappa^\top \mathbf{b}_\kappa)^{-1} \mathbf{b}_\kappa^\top \hat{A}_k - (\mathbf{b}_\kappa^\top \mathbf{b}_\kappa)^{-1} \mathbf{r}_\kappa^\top \boldsymbol{\lambda},$$

where $\boldsymbol{\lambda}$ is a vector of Lagrange multipliers.

This method is implemented in the routine `beed` of **ExtremalDep** and its usage is demonstrated through the analysis of heavy rainfall in France. Hydrologists are interested in identifying different geographic regions that differ from each other in that there are clusters of weather stations whose data exhibit substantially different levels of extreme dependence. Within a cluster, climate characteristics are expected to be homogeneous, whereas they can be quite heterogeneous between clusters. The dataset is available through the `PrecipFrance` object which consists of weekly maxima of hourly rainfall (`$precip`) recorded at 92 weather stations in France, during the Fall season between 1993 and 2011, yielding a sample size of $k = 228$ observations. Coordinates of each station are stored in the list elements `$lat` and `$lon`. Note that hourly rainfall has been appropriately pre-processed and with them the weekly maxima have been already computed from [Bernard et al. \(2013\)](#). By applying the algorithm proposed by [Bernard et al. \(2013\)](#) to the weekly maxima of hourly rainfall, the weather stations are divided into 7 clusters. This is obtained using the `PAMfmado` routine through the following commands

```
R> data(PrecipFrance)
R> attach(PrecipFrance)

R> nclust <- 7
R> PAMfmado <- PAMfmado(precip, nclust)
```

For each cluster, 5 stations are randomly selected in order to have equal size ($d = 5$) clusters and for each group, the Pickands dependence function is estimated using the Bernstein projection estimator based on the madogram with polynomial degree equal $k = 7$. To summarise, an estimate of the extremal coefficient is computed using (2.7), i.e. $\hat{\eta}_k = 5\tilde{A}_{k,\kappa}(1/5, \dots, 1/5)$, through the following commands

```
R> clust <- PAMmado$clustering
R> d <- 5
R> stationsn <- matrix(NA, nclust, d)
R> xx <- simplex(d=d, n=15)
R> fit <- list(length=nclust)
R> est <- vector(length=nclust)
R> set.seed(1)
R> for(i in 1:nclust){
+   stationsn[i,] <- sample(which(clust==i), 5)
+   data_tmp <- precip[,stationsn[i,]]
+   data_uf_tmp <- trans2UFrechet(data_tmp, type="Empirical")
+   fit[[i]] <- beed(data_uf_tmp, xx, d, "md", "emp", k=7)
+   est[i] <- fit[[i]]$extind
+ }
```

The left panel of Figure 3 indicates the extremal dependence is strongest in the center of the country, away from the coasts, where the conjunction of different densities of air masses produces extreme rain storms. This is consistent with what climatologists expect since extreme precipitation that affects the Mediterranean coast in the fall is caused by the interaction of southern and mountain winds coming from the Pyrénées, Cévennes and Alps regions. In the north, heavy rainfall is produced by mid-latitude perturbations in Brittany or regions further north and Paris. Within clusters, extremes are strongly dependent. The right panel of Figure 3 shows the pairwise extremal coefficients from all 92 stations, computed through the estimated Pickands dependence functions using the raw madogram estimator (MD) and its Bernstein projection (MD-BP), versus the geodesic distance between sites. We have $\hat{\eta}_k \leq 1.5$ for the locations that are less than 200 km apart, meaning that extremes are either strongly or mildly dependent, while for sites more than 200 km apart, we have $\hat{\eta}_k > 1.5$, meaning that extremes are at most weakly dependent or even independent. The graph also shows the benefits of the projection method: after projection, the extremal coefficients fall within the admissible range $[1, 2]$. The `beed` function is used for the MD-PB estimator whereas `madrogram` implements the raw madogram estimator MD. The following set of commands were used for the estimation.

```
R> library(geosphere)

R> pairs <- t(combn(92,2))
R> pairs.LL0 <- cbind(pairs, lon[pairs[,1]], lat[pairs[,1]],
+                   lon[pairs[,2]], lat[pairs[,2]])
R> pairs.dist <- apply(pairs.LL0, 1, function(x) distm(x=x[3:4], y=x[5:6],
+                   fun=distGeo) )/1000

R> pairs.EC <- pairs.ECBP <- vector(length=nrow(pairs))
```

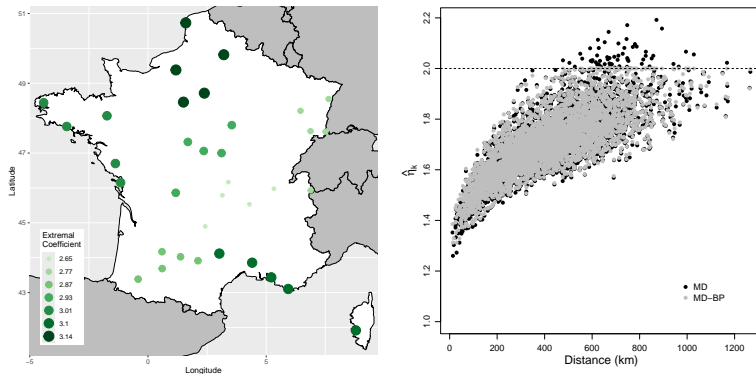


Figure 3: Clusters of 35 weather stations and their estimated extremal coefficients in dimension $d = 5$ using French weekly precipitation maxima (left). Evolution of pairwise extremal coefficients with respect to the distance (right).

```
R> S <- simplex(d=2, n=49)
R> for(i in 1:nrow(pairs)){
+   data.tmp <- trans2UFrechet(precip[,pairs[i,]], type="Empirical")
+   fit.tmp <- beed(data.tmp, S, 2, "md", "emp", k=7)
+   pairs.ECBP[i] <- fit.tmp$extind
+   pairs.EC[i] <- 2*madogram(S, data.tmp, "emp")[which(S[,1]==0.5)]
+ }
```

2.4.2 Bernstein polynomials modeling and Bayesian nonparametric inference

In many applications it is crucial to estimate joint probabilities such as $p = \mathbb{P}(Y_1 > y_1, Y_2 > y_2)$, for pair of extreme values value (y_1, y_2) which allows the estimation of related quantities such as small conditional probabilities $\mathbb{P}(Y_j > y_j | Y_i > y_i)$ with $i, j = 1, 2$. Section 2.1 describes a theoretical framework that can be used to approximate such probabilities and we now briefly describe a Bayesian nonparametric inference method based on Bernstein polynomials introduced by Marcon et al. (2016).

Let $\mathbf{y}_1, \dots, \mathbf{y}_k$ be k (independent) observations (approximately) distributed as a bivariate GEV distribution. First, a prior distribution on the parameters $\boldsymbol{\theta}_j = (\mu_j, \sigma_j, \gamma_j)^\top, j = 1, 2$, of the marginal GEV distributions is specified as $\Pi(\boldsymbol{\theta}_j) = \Pi(\mu_j)\Pi(\sigma_j)\Pi(\gamma_j) \propto 1/\sigma_j$ with $\sigma_j > 0$, i.e. a product of uniform prior distributions on the real line for $\mu_j, \log(\sigma_j)$ and γ_j . Note that this improper prior distribution leads to a proper posterior distribution (Northrop and Attalides, 2016). Samples from the posterior distribution are generated using an adaptive (Gaussian) random-walk Metropolis-Hastings (RWMH) algorithm (Haario et al., 2001; Garthwaite et al., 2016). At the current state s of the chain, $\boldsymbol{\theta}_j^{(s)}$ is updated by the proposal $\boldsymbol{\theta}'_j \sim \phi_3(\boldsymbol{\theta}^{(s)}, \tau^{(s)}\Sigma^{(s)})$, where $\phi_d(\mathbf{a}, A)$ is a d -dimensional Gaussian density with mean \mathbf{a} and covariance A . The proposal covariance matrix $\Sigma^{(s)}$ is specified as

$$\Sigma^{(s+1)} = \begin{cases} (1 + [\tau^{(s)}]^2/s)\mathbb{I}_3, & s \leq 100 \\ \frac{1}{s-1} \sum_{l=1}^s (\boldsymbol{\theta}^{(l)} - \bar{\boldsymbol{\theta}}^{(s)})(\boldsymbol{\theta}^{(l)} - \bar{\boldsymbol{\theta}}^{(s)})^\top + \{(\tau^{(s)})^2/s\}\mathbb{I}_3, & s > 100, \end{cases} \quad (2.14)$$

where \mathbb{I}_d is the d -dimensional identity matrix, $\bar{\boldsymbol{\theta}}^{(s)} = s^{-1}(\boldsymbol{\theta}^{(1)} + \dots + \boldsymbol{\theta}^{(s)})$, and $\tau^{(s)} > 0$ is a scaling parameter that affects the acceptance rate of proposal parameter values (Haario et al.,

2001) and, τ is updated using a Robbins-Monro process so that

$$\log \tau^{(s+1)} = \log \tau^{(s)} + c(\pi^{(s)} - \pi^*), \quad (2.15)$$

where $c = (2\pi)^{1/2} \exp(\zeta_0^2/2)/(2\zeta_0)$ is a steplength constant, $\zeta_0 = -1/\Phi(\pi^*/2)$, and Φ is the univariate standard Gaussian distribution function (Garthwaite et al., 2016). To control the desired sampler acceptance probability, the parameter $\pi^* = 0.234$ is specified as in Roberts et al. (1997).

In the bivariate case, the polynomial Pickands dependence function in Bernstein form becomes

$$A_\kappa(t | \boldsymbol{\beta}_\kappa) := \sum_{j=0}^{\kappa} \beta_j b_j(t; \kappa), \quad t \in \mathcal{R},$$

for $\kappa = 0, 1, \dots$, where $\boldsymbol{\beta}_\kappa = (\beta_0, \dots, \beta_\kappa)^\top$ and the polynomial basis in (2.13) reduces to

$$b_j(t; \kappa) = \frac{\kappa!}{j!(\kappa-j)!} j^j (1-j)^{\kappa-j}, \quad j = 0, \dots, \kappa.$$

For fixed degree κ , Marcon et al. (2016) derived the restrictions on $\boldsymbol{\beta}_\kappa$ so that A_κ satisfies conditions (C2)-(C3) and is therefore a valid Pickands dependence function. They also demonstrated that the polynomial A_κ implies that the distribution of the corresponding angular measure can be written as a Bernstein polynomial of degree $\kappa - 1$,

$$H_{\kappa-1}([0, w] | \boldsymbol{\eta}_\kappa) := \begin{cases} \sum_{j \leq \kappa-1} \eta_j b_j(w; \kappa-1) & \text{if } w \in [0, 1), \\ 1 & \text{if } w = 1, \end{cases} \quad (2.16)$$

where $\boldsymbol{\eta}_\kappa = (\eta_0, \dots, \eta_{\kappa-1})^\top$. Additionally, Marcon et al. (2016) established the conditions on the coefficients $\boldsymbol{\eta}_\kappa$ so that $H_{\kappa-1}$ is the distribution of a valid angular measure and proposed a Bayesian nonparametric procedure for the inference of both A_κ and $H_{\kappa-1}$, which can then be used to compute an approximation of joint tail probabilities. The proposed method consists of three main steps: 1) the specification of a prior distribution for the polynomial order and coefficients $(\kappa, \boldsymbol{\eta}_\kappa)$, 2) the derivation of the likelihood function, 3) the definition of a Markov Chain Monte Carlo (MCMC) algorithm for the posterior distribution computation. In particular, $\Pi(\kappa, \boldsymbol{\eta}_\kappa) = \Pi(\boldsymbol{\eta}_\kappa | \kappa) \Pi(\kappa)$, where $\Pi(\kappa)$ is a prior on the polynomial order (e.g., Poisson, negative Binomial, etc.) and $\Pi(\boldsymbol{\eta}_\kappa | \kappa) = \Pi(\eta_1, \dots, \eta_{\kappa-2} | p_1, p_0, \kappa) \Pi(p_1 | \kappa, p_0) \Pi(p_0)$ is a prior on the coefficients $\boldsymbol{\eta}_\kappa$, where $\Pi(p_1 | \kappa, p_0)$ and $\Pi(p_0)$ are the priors on the coefficients representative of the atoms $\eta_0 = p_0$ and $\eta_{\kappa-1} = 1 - p_1$ at the edges of the interval $[0, 1]$. Such priors are specified as uniform distributions on suitable intervals, which have been chosen to ensure that the resulting Bernstein polynomial satisfies the constraint (C1). Specification of the prior $\Pi(\boldsymbol{\eta}_\kappa | \kappa)$ induces also a prior on the coefficients $\boldsymbol{\beta}_\kappa$ of the corresponding polynomial $A_\kappa(t | \boldsymbol{\beta}_\kappa)$, which automatically satisfy constraints (C2)-(C3). To deal with the fact at each MCMC iteration the dimension of $\boldsymbol{\theta}_{t\kappa}$ changes with κ , a trans-dimensional MCMC scheme is considered following Marcon et al. (2016). At the state s , $(\boldsymbol{\eta}_{\kappa^{(s)}}^{(s)}, \kappa^{(s)})$ is updated using the proposal distribution $q(\boldsymbol{\eta}_\kappa, \kappa | \boldsymbol{\eta}_{\kappa^{(s)}}^{(s)}, \kappa^{(s)}) = \Pi_{\boldsymbol{\eta}}(\boldsymbol{\eta}_\kappa | \kappa) q_\kappa(\kappa | \kappa^{(s)})$, where $q_\kappa(\kappa | \kappa^{(s)})$ is defined such that if $\kappa^{(s)} = 3$, it places mass on $\kappa = 4$ with probability 1 and if $\kappa^{(s)} > 3$ it places mass on $\kappa^{(s)} - 1$ and $\kappa^{(s)} + 1$ with equal probability. Finally, the likelihood function is defined as $\mathcal{L}(\boldsymbol{\vartheta}) = \prod_{i=1}^m \mathcal{L}(y_i | \boldsymbol{\vartheta})$, where $\boldsymbol{\vartheta} = (\boldsymbol{\theta}_1^\top, \boldsymbol{\theta}_2^\top, \boldsymbol{\beta}_\kappa^\top, \kappa)^\top$ and for any y_j such that $(1 + \gamma_j(y_j - \mu_j)/\sigma_j) > 0$ with $j = 1, 2$,

$$\mathcal{L}(\boldsymbol{y} | \boldsymbol{\vartheta}) = G_{\boldsymbol{\theta}}(\boldsymbol{y} | A_\kappa(t | \boldsymbol{\beta}_\kappa)) \{ (A_\kappa(t | \boldsymbol{\beta}_\kappa) - t A'_\kappa(t | \boldsymbol{\beta}_\kappa)) (A_\kappa(t | \boldsymbol{\beta}_\kappa) - (1-t) A'_\kappa(t | \boldsymbol{\beta}_\kappa)) \}$$

Algorithm 1: Trans-dimensional MCMC scheme

1 **Initialize:** Set $\boldsymbol{\vartheta}^{(0)} = (\boldsymbol{\theta}_1^{(0)}, \boldsymbol{\theta}_2^{(0)}, \kappa^{(0)}, \boldsymbol{\eta}_{\kappa^{(0)}}^{(0)})$, $\boldsymbol{\eta}_{\kappa^{(0)}}^{(0)}$, $\tau_i^{(0)}$ and $\Sigma_i^{(0)}$ for $j = 1, 2$.
 2 **for** $s = 0$ **to** M **do**
 3 **Step 1:** *Marginal component 1:*
 4 Draw proposal $\boldsymbol{\theta}'_1 \sim MVN(\boldsymbol{\theta}_1^{(s)}, \tau_1^{(s)} \Sigma_1^{(s)})$.
 5 Compute acceptance probability $\pi_1 = \min \left(\frac{\mathcal{L}(\boldsymbol{\theta}'_1, \boldsymbol{\theta}_2^{(s)}, \kappa^{(s)}, \boldsymbol{\beta}_{\kappa^{(s)}}^{(s)}) \Pi(\boldsymbol{\theta}'_1)}{\mathcal{L}(\boldsymbol{\theta}_1^{(s)}, \boldsymbol{\theta}_2^{(s)}, \kappa^{(s)}, \boldsymbol{\beta}_{\kappa^{(s)}}^{(s)}) \Pi(\boldsymbol{\theta}_1^{(s)})}, 1 \right)$.
 6 Draw $U_1 \sim \mathcal{U}(0, 1)$. If $\pi_1 < U_1$ then set $\boldsymbol{\theta}_1^{(s+1)} = \boldsymbol{\theta}'_1$ else set $\boldsymbol{\theta}_1^{(s+1)} = \boldsymbol{\theta}_1^{(s)}$.
 7 Update $\Sigma_1^{(s)}$ according to (2.14).
 8 Update $\tau_1^{(s)}$ according to (2.15).
 9 **Step 2:** *Marginal component 2:*
 10 Draw proposal $\boldsymbol{\theta}'_2 \sim MVN(\boldsymbol{\theta}_2^{(s)}, \tau_2^{(s)} \Sigma_2^{(s)})$.
 11 Compute acceptance probability $\pi_2 = \min \left(\frac{\mathcal{L}(\boldsymbol{\theta}_1^{(s+1)}, \boldsymbol{\theta}'_2, \kappa^{(s)}, \boldsymbol{\beta}_{\kappa^{(s)}}^{(s)}) \Pi(\boldsymbol{\theta}'_2)}{\mathcal{L}(\boldsymbol{\theta}_1^{(s+1)}, \boldsymbol{\theta}_2^{(s)}, \kappa^{(s)}, \boldsymbol{\beta}_{\kappa^{(s)}}^{(s)}) \Pi(\boldsymbol{\theta}_2^{(s)})}, 1 \right)$.
 12 Draw $U_2 \sim \mathcal{U}(0, 1)$. If $\pi_2 < U_2$ then set $\boldsymbol{\theta}_2^{(s+1)} = \boldsymbol{\theta}'_2$ else set $\boldsymbol{\theta}_2^{(s+1)} = \boldsymbol{\theta}_2^{(s)}$.
 13 Update $\Sigma_2^{(s)}$ according to (2.14).
 14 Update $\tau_2^{(s)}$ according to (2.15).
 15 **Step 3:** *Dependence structure:*
 16 Draw proposal $\kappa' \sim q_{\kappa}(\kappa | \kappa^{(s)})$ and $\boldsymbol{\eta}'_{\kappa'} \sim q_{\eta}(\boldsymbol{\eta}_{\kappa} | \kappa')$, and compute $\boldsymbol{\eta}'_{\kappa'}$.
 17 Set $c = 1/2$ if $\kappa^{(s)} = 3$ or $c = 1$ if $\kappa^{(s)} > 3$.
 18 Compute acceptance probability $\pi_3 = \min \left(c \frac{\Pi(\kappa')}{\Pi(\kappa^{(s)})} \frac{\mathcal{L}(\boldsymbol{\theta}_1^{(s+1)}, \boldsymbol{\theta}_2^{(s+1)}, \kappa', \boldsymbol{\beta}_{\kappa'}^{(s)})}{\mathcal{L}(\boldsymbol{\theta}_1^{(s+1)}, \boldsymbol{\theta}_2^{(s+1)}, \kappa^{(s)}, \boldsymbol{\beta}_{\kappa^{(s)}}^{(s)})}, 1 \right)$.
 19 Draw $U_3 \sim \mathcal{U}(0, 1)$. If $\pi_3 < U_3$ then set $\kappa^{(s+1)} = \kappa'$, $\boldsymbol{\eta}_{\kappa^{(s+1)}}^{(s+1)} = \boldsymbol{\eta}'_{\kappa'}$, $\boldsymbol{\beta}_{\kappa^{(s+1)}}^{(s+1)} = \boldsymbol{\beta}'_{\kappa'}$
 else set $\kappa^{(s+1)} = \kappa^{(s)}$, $\boldsymbol{\eta}_{\kappa^{(s+1)}}^{(s+1)} = \boldsymbol{\eta}_{\kappa^{(s)}}^{(s)}$, $\boldsymbol{\beta}_{\kappa^{(s+1)}}^{(s+1)} = \boldsymbol{\beta}_{\kappa^{(s)}}^{(s)}$.

$$+ \frac{t(1-t)}{r} A''_{\kappa}(t | \boldsymbol{\beta}_{\kappa}) \left. \right\} \frac{1}{\sigma_1 \sigma_2} \left(1 + \gamma_1 \frac{y_1 - \mu_1}{\sigma_1} \right)^{-1/\gamma_1 - 1} \left(1 + \gamma_2 \frac{y_2 - \mu_2}{\sigma_2} \right)^{-1/\gamma_2 - 1}$$

and where $\boldsymbol{\theta} = (\boldsymbol{\theta}_1^{\top}, \boldsymbol{\theta}_2^{\top})^{\top}$, $t = z_2/r$, $r = z_1 + z_2$, see Marcon et al. (2016) and Beranger et al. (2021) for details. The MCMC scheme for the joint inference of marginal distribution and extremal dependence is reported in Algorithm 1. For pairs (y_1^*, y_2^*) of future unobserved yet extremes values, the joint exceeding probability can be estimated through the Bayesian paradigm using the posterior predictive distribution which can be approximated, given a sample $\boldsymbol{\vartheta}_i$ with $i = 1, \dots, M$, from the posterior distribution as

$$\begin{aligned}
 \mathbb{P}(Z_1 > z_1^*, Z_2 > z_2^*) &\approx 2 \sum_{i=1}^M \frac{1}{\kappa_i} \sum_{j=0}^{\kappa_i - 2} (\eta_{i,j+1} - \eta_{i,j}) \\
 &\times \left(\frac{(j+1) \text{B}(z_1^*/(z_1^* + z_2^*) | j+2, \kappa_i - j - 1)}{z_1^*} \right)
 \end{aligned} \tag{2.17}$$

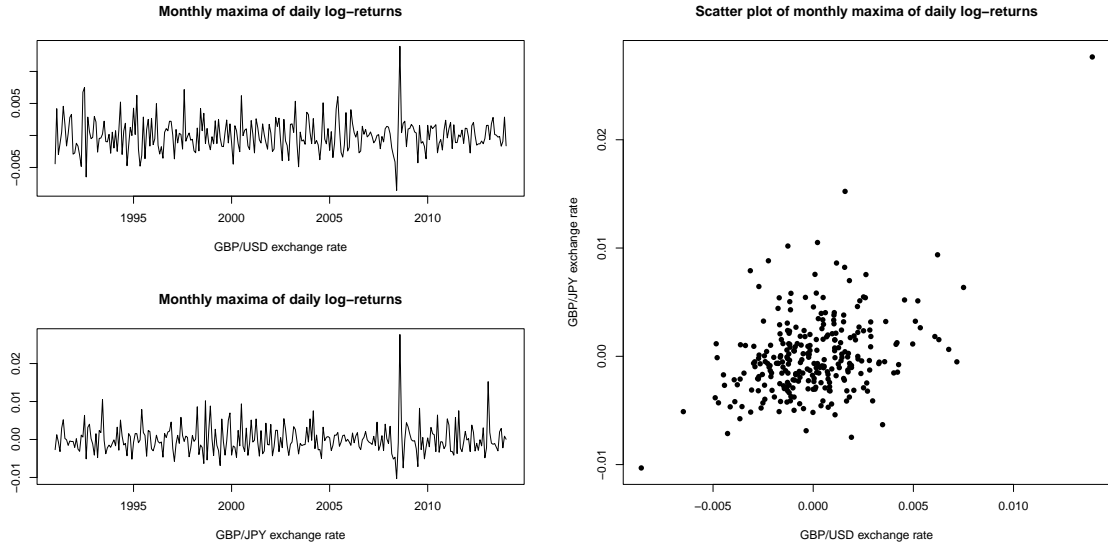


Figure 4: De-trended and de-seasonalised times series of monthly-maxima of log-returns of GBP/USD and GBP/JPY exchange rates (left) and corresponding scatterplot (right).

$$+ \frac{(k_i - j - 1) B(z_2^*/(z_1^* + z_2^*) | \kappa_i - j, j + 1)}{z_2^*},$$

where (Z_1, Z_2) are distributed as a bivariate GEV with unit-Fréchet margins, $z_j^* = \sum_{i=1}^M (1 + \gamma_{i,j}(y_j^* - \mu_{i,j})/\sigma_{i,j})^{1/\gamma_{i,j}}$ with $j = 1, 2$ and $B(x | a, b)$, $x \in [0, 1]$, denotes the distribution function of a Beta random variable with shape parameters $a, b > 0$ (see [Marcon et al., 2016](#), for details).

We show the utility of the methodology by analyzing the joint extremal behavior of log-returns of exchange rates between Pound Sterling and U.S. Dollar (GBP/USD), and Pound Sterling and Japanese Yen (GBP/JPY). The data is available as `logReturns` and consists of the monthly maxima of daily log-returns exchange rates from March 1991 to December 2014 (286 observations). Exchange rates are `$USD` and `$JPY`, while `$date_USD` and `$date_JPY` are the date when the monthly maxima was attained. First the trend and seasonality are removed from each maxima series using the `ts()` and `stl()` functions from the `stats` package.

```
R> data(logReturns)
R> mm_gbp_usd <- ts(logReturns$USD, start=c(1991,3), end=c(2014,12), frequency=12)
R> mm_gbp_jpy <- ts(logReturns$JPY, start=c(1991,3), end=c(2014,12), frequency=12)

R> seas_usd <- stl(mm_gbp_usd, s.window="period")
R> seas_jpy <- stl(mm_gbp_jpy, s.window="period")

R> mm_gbp_usd_filt <- mm_gbp_usd - rowSums(seas_usd$time.series[, -3])
R> mm_gbp_jpy_filt <- mm_gbp_jpy - rowSums(seas_jpy$time.series[, -3])
```

The top-left and bottom-left panels of Figure 4 display the de-trended and de-seasonalised maxima and the right panel scatter plot shows strong dependence between the extremes of both exchanges rates. The extremal dependence structure is estimated using the Bayesian

nonparametric framework described above. The `fExtDep.np` routine allows for nonparametric estimation of the extremal dependence and `method = "Bayesian"` specifies that such a dependence is in Bernstein polynomial form and a Bayesian approach is used for the inference. The argument `mar.fit = TRUE` (default) allows for joint estimation of the margins and dependence while `mar.prelim = TRUE` (default) fits the marginal distributions using the RWMH algorithm and the `fGEV` routine, in order to obtain starting values for the marginal parameters. The prior distribution for κ is set to be a negative binomial on $\kappa-3$ with mean 3.2 and variance 4.48, and for the point masses p_0 and p_1 uniform distributions on $[0, 0.5]$ and $[a, b]$ respectively, where $a = \max\{0, (\kappa-1)p_0 - \kappa/2 + 1\}$ and $b = (p_0 + \kappa/2 - 1)/(\kappa-1)$. Below, only the hyper-parameters need to be specified since `prior.k="nbinom"` and `prior.pm="unif"` by default. Lastly, a two-column object `mm_gbp` representing the data is created.

```
R> hyperparam <- list(mu.nbinom = 3.2, var.nbinom = 4.48)
R> mm_gbp <- cbind(as.vector(mm_gbp_usd_filt), as.vector(mm_gbp_jpy_filt))
R> set.seed(123)
R> gbp_mar <- fExtDep.np(method="Bayesian", data=mm_gbp,
+                       par10=rep(0.1, 3), par20=rep(0.1,3),
+                       sig10=0.0001, sig20=0.0001, k0=5,
+                       hyperparam = hyperparam, nsim=5e+4)
```

Preliminary on margin 1

```
|=====| 100%
```

Preliminary on margin 2

```
|=====| 100%
```

Estimation of the extremal dependence and margins

```
|=====| 100%
```

```
R> diagnostics(gbp_mar)
```

The `gbp_mar` object contains the posterior samples for all the parameters: point mass p_0 and p_1 , polynomial coefficients $\boldsymbol{\eta}$ and degree κ , marginal parameters $\boldsymbol{\theta}_1$ and $\boldsymbol{\theta}_2$, respectively reported by the arguments `pm`, `eta`, `k`, `mar1` and `mar2`. Its also contains binary vectors indicating the accepted marginal and dependence proposals (`accepted.mar1`, `accepted.mar2` and `accepted`) and the marginal proposals that were rejected right away for not being in the parameter space (`straight.reject1` and `straight.reject2`). It also includes acceptance probabilities at each step (`acc.vec`, `acc.vec.mar1` and `acc.vec.mar2`), the marginal scaling parameters τ_1 and τ_2 (`sig1.vec` and `sig2.vec`), as well as some of the inputs. The `diagnostics` function investigates the convergence of the algorithm, producing Figure 5. The top panels display the scaling parameters τ_1 and τ_2 from the marginal proposals and the polynomial degree κ , as function of the iterations. The bottom panels show the corresponding acceptance probability with the desired acceptance probability of 0.234 (horizontal black solid lines). Overall, Figure 5 suggests a burn-in period of 30,000 iterations. The `summary.ExtDep` routine computes summary statistics of the MCMC output, including posterior sample, mean and 95% credibility intervals (can be modified using argument `cred`) for the angular density and Pickands dependence function. Posterior mean and credibility intervals are also

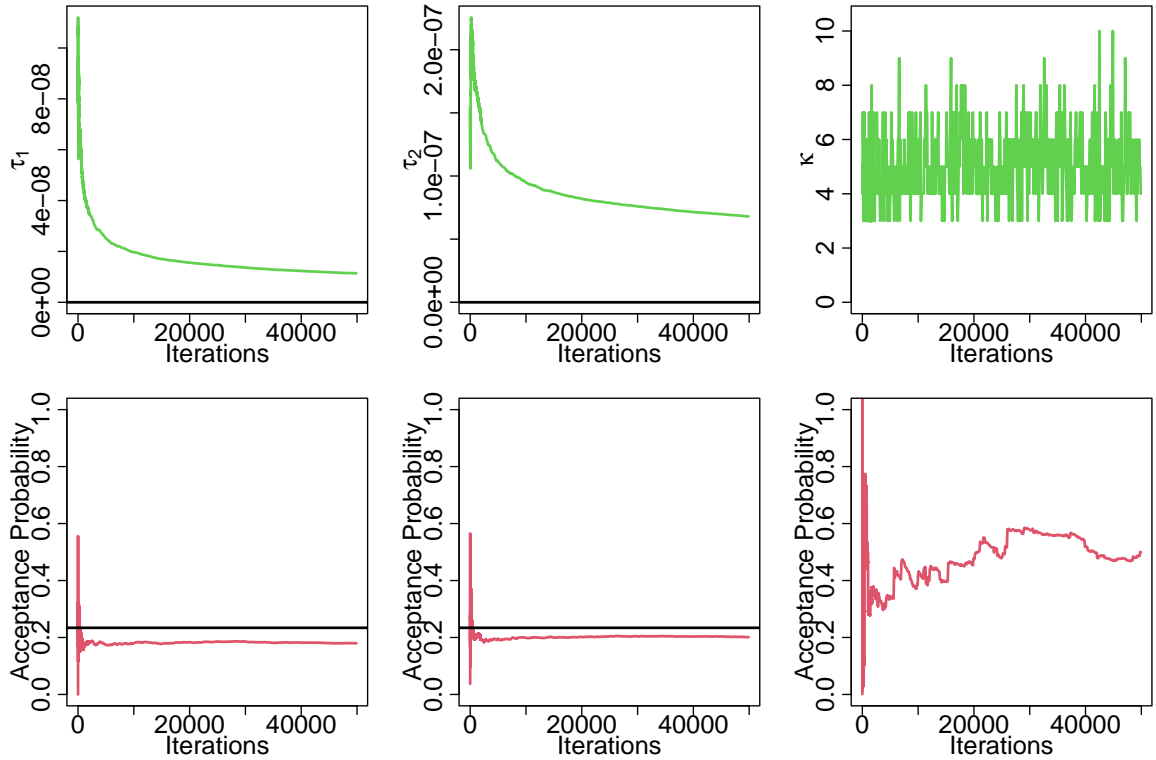


Figure 5: Diagnostic plots for the MCMC algorithm. Left and centre columns focus on the marginal components, illustrating the respective sampler scaling parameter and acceptance probability. Right column focuses on the dependence structure, illustrating the value of the polynomial degree throughout the algorithm and acceptance probability.

computed for all parameters. Setting `plot=TRUE` displays the posterior mean and credibility intervals for both angular density and Pickands dependence function, as well as the prior and posterior distribution for the point mass p_0 and the polynomial degree κ . The `returns` routine inputs the outputs of the `fExtDep.np` and `summary.ExtDep` (via the arguments `out` and `summary.mcmc`) to compute exceeding probabilities as defined in (2.17), for extreme values specified by y . The argument `plot` allows to visualize such probabilities as long as y defines a square grid and `data` adds the relevant datapoints. Usage of the `summary.ExtDep` and `returns` functions is provided below with graphical outputs presented in Figure 6.

```
R> gbp_mar_sum <- summary.ExtDep(mcmc=gbp_mar, burn=30000, plot=TRUE)

R> mm_gbp_range <- apply(mm_gbp,2,quantile,c(0.9,0.995))

R> y_gbp_usd <- seq(from=mm_gbp_range[1,1], to=mm_gbp_range[2,1], length=20)
R> y_gbp_jpy <- seq(from=mm_gbp_range[1,2], to=mm_gbp_range[2,2], length=20)
R> y <- as.matrix(expand.grid(y_gbp_usd, y_gbp_jpy, KEEP.OUT.ATTRS = FALSE))

R> ret_marg <- returns(out=gbp_mar, summary.mcmc=gbp_mar_sum, y=y,
+                      plot=TRUE, data=mm_gbp,
```

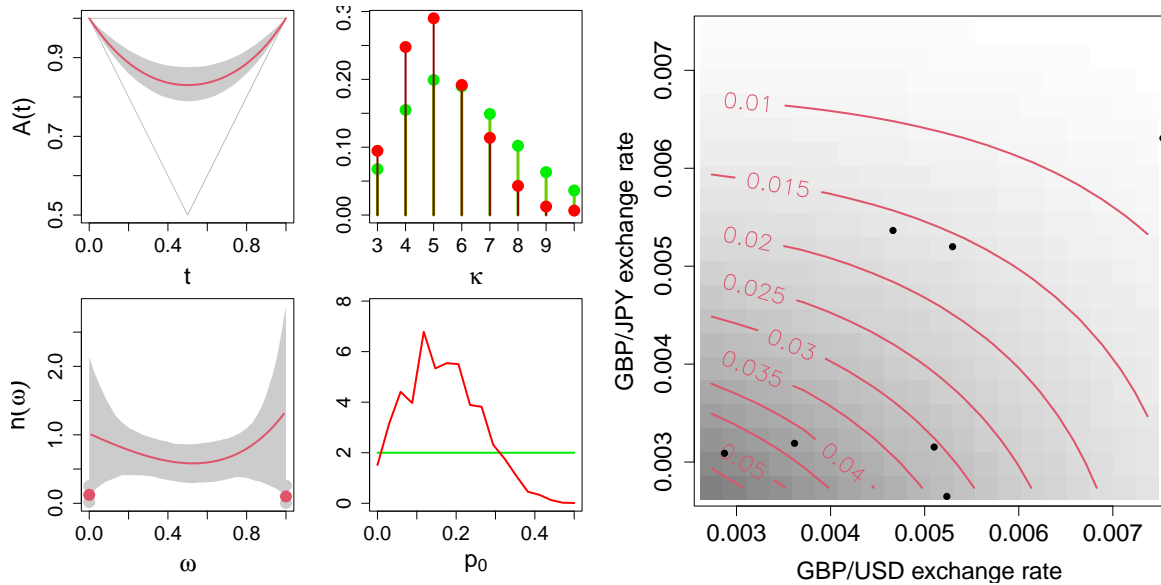


Figure 6: Outputs of the `summary.ExtDep` (left) and `returns` (right) functions.

```
+ labels=c("GBP/USD exchange rate", "GBP/JPY exchange rate"))
```

As mentioned at the beginning of this section, computing small conditional probabilities such as $\mathbb{P}(\text{GBP/USD} > q_1 | \text{GBP/JPY} > q_2)$ or $\mathbb{P}(\text{GBP/JPY} > q_2 | \text{GBP/USD} > q_1)$ can be of interest. To proceed, take $(q_1, q_2) \approx (0.0069, 0.0102)$ which corresponds to the observed 99% quantiles. The joint probability of exceedance is computed (through `returns`) using the approximation $\mathbb{P}(\text{GBP/USD} > q_1, \text{GBP/JPY} > q_2) \approx \mathbb{P}(Z_1 > z_1^*, Z_2 > z_2^*) \approx 0.0149$, where z_1^* and z_2^* are the transformation of q_1 and q_2 to unit Fréchet scale. Using the `pGEV` function to evaluate the marginal probability of exceedance, we obtain $\mathbb{P}(\text{GBP/USD} > q_1 | \text{GBP/JPY} > q_2) \approx 0.3491$ and $\mathbb{P}(\text{GBP/JPY} > q_2 | \text{GBP/USD} > q_1) \approx 0.4152$. The computations are presented in the code below.

```
R> qs <- apply(mm_gbp, 2, quantile, c(0.99))
R> jointP <- returns(out=gbp_mar, summary.mcmc=gbp_mar_sum,
+ y=matrix(qs, ncol=2) )
par1 <- gbp_mar_sum$mar1.mean
par2 <- gbp_mar_sum$mar2.mean
jointP / pGEV(qs[1], loc=par1[1], scale=par1[2], shape=par1[3], lower.tail=F)
jointP / pGEV(qs[2], loc=par2[1], scale=par2[2], shape=par2[3], lower.tail=F)
```

2.4.3 Simulation of extreme values

In environmental statistics, there is active research in “stochastic weather generators” which aims at simulating realisations from atmospheric variables according to some stochastic representation. A challenging task is the simulation of high-dimensional extremes, since their extremal dependence (Pickands dependence function or angular measure) is an infinite dimensional parameter of the multivariate GEV distribution and is therefore challenging to estimate. The ability to simulate high-dimensional extremes permits to approximate the tail probabilities in (2.8) and (2.9), even though few extremes are available in the dataset.

For simplicity, most of the simulation methods assume that the extremal dependence complies with some parameter model, while few attempt to consider a nonparametric approach. [Marcon et al. \(2017\)](#) proposed a flexible procedure for sampling from bivariate extremes with a semiparametric dependence structure, which is summarized as follows. For every small probabilities p_1 and p_2 such that $L(p_1, p_2) \in [0, 1]$ and $R(p_1, p_2) \in [0, 1]$, the tail probabilities in (2.8) and (2.9) can be approximated by $\mathbb{P}(X_1 > Q_1(p_1) \text{ or } X_2 > Q_2(p_2)) \approx L(p_1, p_2)$ and $\mathbb{P}(X_1 > Q_1(p_1) \text{ and } X_2 > Q_2(p_2)) \approx R(p_1, p_2)$. For such probabilities p_1 and p_2 , we have that $L(p_1, p_2) = 2\mathbb{E}(\max(p_1 W, p_2(1 - W)))$ and $R(p_1, p_2) = 2\mathbb{E}(\min(p_1 W, p_2(1 - W)))$, where W is a random variable on $[0, 1]$ distributed according to the angular distribution H . Now, let $(Z_1, Z_2) = R(W, 1 - W)$, where R is a unit-Pareto random variable, then $\mathbb{P}(Z_1 > z_1 \text{ or } Z_2 > z_2) = 2\mathbb{E}(\max(W/z_1, (1 - W)/z_2))$ and $\mathbb{P}(Z_1 > z_1 \text{ and } Z_2 > z_2) = 2\mathbb{E}(\min(W/z_1, (1 - W)/z_2))$. [Marcon et al. \(2017\)](#) proposed to model H through Bernstein polynomials and demonstrated that H can be written as a finite mixture of Beta distributions with weights defined by a suitable transformation of the polynomial coefficients. This led to a simple algorithm to sample from H (see Algorithm 1) and an algorithm for sampling observations from the tail of a bivariate distribution (see Algorithm 3), which can be used to approximate the corresponding tail probabilities. Briefly, from (2.6) we have that for a sufficiently large n and a sufficiently small $p_j = p_{n,j}$ (with $p_j \rightarrow 0$ as $n \rightarrow \infty$), $Q_j(p_j) \approx \mu_j + \gamma_j((np_j)^{-\gamma_j} - 1)/\sigma_j$, with $j = 1, 2$. Let u_1 and u_2 be two high thresholds such that for every p_1 and p_2 for which the above approximations hold, as well as $L(p_1, p_2) \in [0, 1]$ and $R(p_1, p_2) \in [0, 1]$, we have $Q_j(p_j) > u_j$, $j = 1, 2$. For the failure regions $\mathcal{A}_{\mathbf{u}} = \{(v_1, v_2) : v_1 > u_1 \text{ or } v_2 > u_2\}$ and $\mathcal{B}_{\mathbf{u}} = \{(v_1, v_2) : v_1 > u_1 \text{ and } v_2 > u_2\}$ we have $\mathbb{P}(\mathbf{X} \in \mathcal{A}_{\mathbf{u}}) \approx \mathbb{P}(Z_1 > u_1^* \text{ or } Z_2 > u_2^*)$ and $\mathbb{P}(\mathbf{X} \in \mathcal{B}_{\mathbf{u}}) \approx \mathbb{P}(Z_1 > u_1^* \text{ and } Z_2 > u_2^*)$, where $u_j^* = (1 + \gamma_j(u_j - \mu_j)/\sigma_j)^{1/\gamma_j}$, for $j = 1, 2$. By simulating a large sample of angular components (w_1, \dots, w_N) from H and radial components (r_1, \dots, r_N) from a unit-Pareto distribution, we compute $z_i = 2(r_i w_i, r_i(1 - w_i))$, for $i = 1, \dots, N$ and estimate of the probability of falling in $\mathcal{A}_{\mathbf{u}}$ and $\mathcal{B}_{\mathbf{u}}$ by

$$\hat{p}_{\mathcal{A}_{\mathbf{u}}} = \frac{1}{N} \sum_{i=1}^N \mathbb{1}(z_{i,1} > u_1^* \text{ or } z_{i,2} > u_2^*), \quad \hat{p}_{\mathcal{B}_{\mathbf{u}}} = \frac{1}{N} \sum_{i=1}^N \mathbb{1}(z_{i,1} > u_1^* \text{ and } z_{i,2} > u_2^*). \quad (2.18)$$

The methodology is illustrated on the **Parçay-Meslay** dataset which consists of daily maxima of hourly wind speed (**WS**) and wind gust (**WG**) in meters per second (m/s) and differential of daily range of the hourly air pressure (**DP**) at sea level in millibars. Measurements are taken in the city of Parçay-Meslay, located in the northwest of France, from July 2004 to July 2013. For this analysis, we focus on positive values of **DP** implying an increase in the daily air pressure level. High air pressure levels are associated with a high content of water vapor in the air which often occurs in stormy weather and leads to strong winds. For brevity, we focus on the relationship between **WS** and **DP**. The GEV parameters are first estimated using the Point Process approach (e.g. [Coles, 2001](#), Ch. 7), implemented in the `fpot` routine of the `evd` package ([Stephenson, 2002](#)), where the observed 90% marginal quantiles are set as suitable thresholds. The margins are transformed to unit-Fréchet scale using the `trans2UFrechet` routine with argument `type="empirical"`, meaning the transformation $y_{i,j} = 1/\{1 - F_{n,j}(x_{i,j})\}$, $i = 1, \dots, n$, $j = 1, 2$ is applied, where $F_{n,j}$ denotes the empirical distribution of the j -th component.

```
R> data(WindSpeedGust)
R> years<- format(ParçayMeslay$time, format="%Y")
R> attach(ParçayMeslay[which(years %in% c(2004:2013)),])
```



```

R> WS_th <- quantile(WS,.9)
R> DP_th <- quantile(DP,.9)

R> pars.WS <- evd::fpot(WS, WS_th, model="pp")$estimate
R> pars.DP <- evd::fpot(DP, DP_th, model="pp")$estimate

R> data_uf <- trans2UFrechets(cbind(WS,DP), type="Empirical")

```

The angular distribution is then estimated using the approximate likelihood approach (see [Beranger and Padoan, 2015](#)). Observations with radius component greater than their 90% quantile are selected and the routine `fExtDep.np` is then called with arguments `method="Frequentist"` and `type="maxima"` to maximize the likelihood of a polynomial angular distribution in Bernstein form through the non-linear optimization routine `nloptr` from the `nloptr` package ([Ypma and Johnson, 2022](#)) subject to constraints established in [Marcon et al. \(2017\)](#). Empirical studies ([Marcon et al., 2017](#)) suggest that the polynomial degree $\kappa = 10$ is enough. When `type="rawdata"`, data are extracted using a threshold on the radial component set by the argument `u` and the likelihood for a sample maxima written as function of the Pickands dependence function in Bernstein form is optimized. In addition, when `mar.fit=TRUE` then marginal empirical transformation to unit Fréchet of the data is applied. The `plot.ExtDep` routine displays graphical summaries (Pickands dependence function and angular density) of the estimated dependence structure (see left and middle panels of [Figure 7](#)). A moderate level of dependence is observed as well as point masses at the vertices. The routine `rExtDep` with arguments `model="semi.bvevd"` and `angular=TRUE` generates pseudo-angles according to Algorithm 1 of [Marcon et al. \(2017\)](#). The right panel of [Figure 7](#) presents a histogram of 1,000 randomly generated angles and point-masses (black triangles), the red line and dots represent the estimated dependence structure.

```

R> rdata <- rowSums(data_uf)
R> r0 <- quantile(rdata, probs=.90)
R> extdata <- data_uf[rdata>=r0,]

R > SP_mle <- fExtDep.np(method="Frequentist", data=extdata, k0=10, type="maxima")
R> plot.ExtDep.np(out=SP_mle, type="summary")

R> SP_wsim <- rExtDep(nsim, model="semi.bvevd", param=SP_mle$Ahat$beta,
+                   angular=TRUE)

```

The routine `rExtDep` performs random generation of bivariate maxima (`model="semi.bvevd"`) and bivariate exceedances (`model="semi.bvexceed"`), according to Algorithm 2 and 3 of [Marcon et al. \(2017\)](#). When `angular=TRUE` solely angular components are generated, no matter the `model` argument, meaning that setting `model="semi.bvexceed"` in the above call of `rExtDep` would produce the same result. The argument `mar` allows for transformations to GEV margins. When `model="semi.bvexceed"`, one can choose to simulate bivariate observations from the failure regions $\mathcal{A}_{\mathbf{u}}$ (`exceed.type="or"`) or $\mathcal{B}_{\mathbf{u}}$ (`exceed.type="and"`), where \mathbf{u} is a suitable threshold specified by `threshold`. The code below generates 200 observations from both failure regions with threshold $\mathbf{u} = (10, 20)$, above the marginal 90% quantiles (see [Figure 8](#) for an illustration).

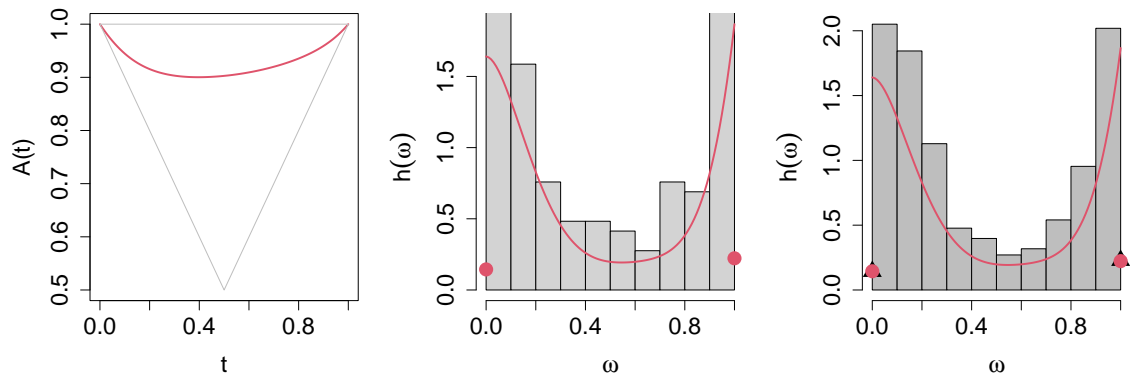


Figure 7: Estimated Pickands dependence function (left) and angular density (middle and right). The middle panel displays the histogram of the data while the right panel displays a histogram of the simulated pseudo-angles as well as the point masses (black triangles).

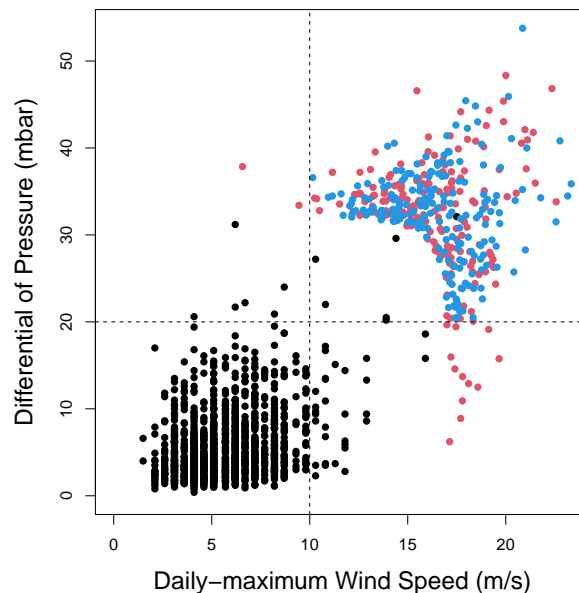


Figure 8: Observed (black dots) differential of pressure (mbar) and daily-maximum wind speed (m/s) in Parçay-Meslay, France between 2004 and 2013. Simulation of 200 observations from the failure regions \mathcal{A}_u (red dots) and \mathcal{B}_u (blue dots) with $\mathbf{u} = (10, 20)$ (dashed lines).

```
R> set.seed(10)
R> SP_exceed_or <- rExtDep(n=200, model="semi.bvexceed", param=SP_mle$Ahat$beta,
+                          mar=rbind(pars.WS, pars.DP), threshold=c(10,20),
+                          exceed.type="or")

R> SP_exceed_and <- rExtDep(n=200, model="semi.bvexceed", param=SP_mle$Ahat$beta,
+                          mar=rbind(pars.WS, pars.DP), threshold=c(10,20),
+                          exceed.type="and")
```

Finally, the routine `pFailure` computes empirical estimates of probabilities of belonging to the failure sets \mathcal{A}_u (`type="or"`) and \mathcal{B}_u (`type="and"`) by applying formula (2.18) on data

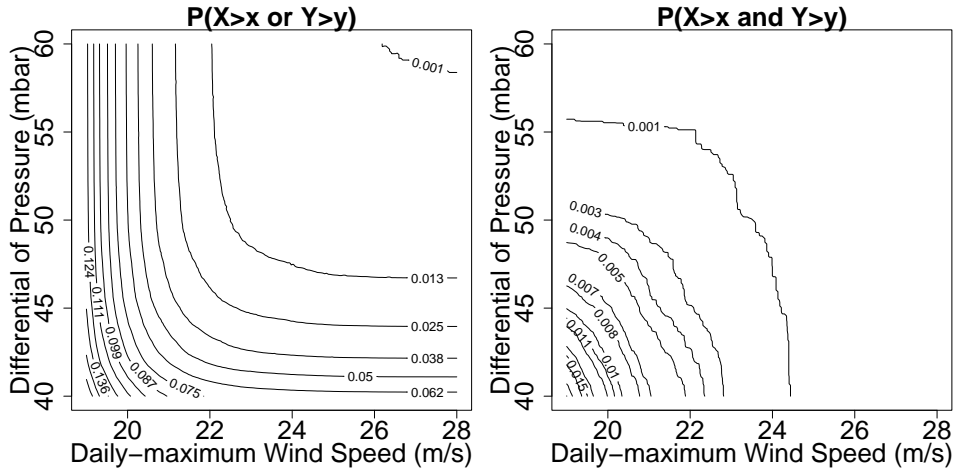


Figure 9: Estimated probabilities to belong to the failure regions \mathcal{A}_u (left) and \mathcal{B}_u (right), for $\mathbf{u} = (u_1, u_2)$, with $18 \leq u_1 \leq 28, 40 \leq u_2 \leq 60$.

generated by `rExtDep`. Both probabilities are computed when `type="both"`. The argument `plot` offers the possibility to display contour plots when sequences of thresholds are provided through the arguments `u1` and `u2`. The following code generates $N = 50,000$ samples to estimate the probabilities of belonging to each failure sets for thresholds ranging from 19 to 28 for the wind speed and from 40 to 60 for the differential of pressure with outputs given in Figure 9.

```
R> pF <- pFailure(n=50000, beta=SP_mle$Ahat$beta,
+               u1=seq(from=19, to=28, length=200), mar1=pars.WS,
+               u2=seq(from=40, to=60, length=200), mar2=pars.DP, type="both",
+               plot=TRUE, xlab="Daily-maximum Wind Speed (m/s)",
+               ylab="Differential of Pressure (mbar)", nlevels=15)
```

2.4.4 Estimation of extreme quantile regions

As highlighted in Section 2.1, an important problem is to define a quantile region \mathcal{Q} as in (2.10), given a very small probability p to fall in it. Given a sample of size N , an extreme quantile region can be defined by the level set \mathcal{Q}_N such that $\mathbb{P}(\mathcal{Q}_N) = p$, where $p = p_N$ satisfies $p \rightarrow 0$ and $Np \rightarrow c > 0$ as $N \rightarrow \infty$. For practical purposes, \mathcal{Q}_N can be approximated by the region $\tilde{\mathcal{Q}}_N$ given in (2.11) which requires estimating the marginal parameters $\boldsymbol{\theta}_j = (\mu_j, \sigma_j, \gamma_j)^\top$, $j = 1, 2$, the basic set S and the density of the angular measure, allowing, in turn, to obtain an estimate of $\xi(S)$. Beranger et al. (2021) discussed a Bayesian approach for the inference of $\tilde{\mathcal{Q}}_N$ based on a polynomial angular measure in Bernstein form and the censored-likelihood approach (e.g. Beirlant et al., 2004, Ch. 8). Since such a methodology is similar to the one described in Section “Bernstein polynomials modeling and Bayesian nonparametric inference”, we refer to Beranger et al. (2021) for a full description.

The methodology is illustrated on the dataset `Milan.winter`, which consists of air pollution levels recorded in Milan, Italy, over the winter period October 31st–February 27/28th, between December 31st 2001 and December 30th 2017. Here we focus on the NO_2 and SO_2

pollutants and use the daily maximum temperature (`MaxTemp`) as covariate. The data is prepared before estimating extreme quantile regions using `fExtDep.np`.

```
R> data(MilanPollution)
R> data <- Milan.winter[,c("NO2", "SO2", "MaxTemp")]
R> data <- data[complete.cases(data),]
```

A quadratic relationship between pollutants and maximum temperature is considered, and the j th marginal mean is written as $\mu_j = \beta_{0,j} + \beta_{1,j}z + \beta_{2,j}t^2$, with $j = 1, 2$, where t is the temperature level. The covariate matrix is defined as

```
R> covar <- cbind(rep(1,nrow(data)), data[,3], data[,3]^2 )
```

which will be provided to `fExtDep.np` through the arguments `cov1` and `cov2`. Since a polynomial angular measure in Bernstein form is considered, we specify a prior distribution for the polynomial degree κ as a negative binomial on $\kappa - 3$ with mean 6 and variance 8 and priors for the point masses p_0 and p_1 respectively as uniform distributions on $[0, 0.2]$ and $[a, b]$, where a and b are defined as in the previous two sections. These are the default prior distributions in the `fExtDep.np` routine, therefore the hyper-parameters are specified by

```
R> hyperparam <- list(mu.nbinom = 6, var.nbinom = 8, a.unif=0, b.unif=0.2)
```

Starting values for the marginal parameters $\theta_j^{(0)} = (\beta_{0,j}^{(0)}, \beta_{1,j}^{(0)}, \beta_{2,j}^{(0)}, \sigma_j^{(0)}, \gamma_j^{(0)})$, $j = 1, 2$, the scaling parameter of the sampler on each margin and the polynomial degree are respectively set by the arguments `par10`, `par20`, `sig10` `sig20` and `k0`. The argument `method="Bayesian"` indicates that a Bernstein polynomial is used to represent the extremal dependence and that the inference part follows the MCMC scheme detailed in [Beranger et al. \(2021, Algorithm 1\)](#). The argument `u=TRUE` specifies that a censored likelihood approach is applied on raw data with threshold `u` set to the marginal 90% quantile by default. Recall that by default the marginal distributions are fitted jointly with the dependence (`mar.fit=TRUE`) but `mar.prelim=FALSE` indicates that no initial marginal fit is required.

```
R> pollut <- fExtDep.np(method="Bayesian", data = data[,-3], u=TRUE,
+                       cov1 = covar, cov2 = covar, mar.prelim=FALSE,
+                       par10 = c(100,0,0,35,1), par20 = c(20,0,0,20,1),
+                       sig10 = 0.1, sig20 = 0.1, k0 = 5,
+                       hyperparam = hyperparam, nsim = 15e+3)
```

U set to 90% quantile by default on both margins

Estimation of the extremal dependence and margins

```
|=====| 100%
```

The output of the estimation procedure can be visualised and summarised using `plot.ExtDep.np` and `summary.ExtDep` by specifying the arguments `type="Qsets"`, `out` and `summary.mcmc`. Since covariates are used to model the marginal parameters, we need to provide the covariate levels at which the extreme quantile regions will be computed. In this example, extreme quantile regions are computed at the minimum, median and maximum of the observed daily maximum temperatures. The covariate matrices `QatCov1` and `QatCov2` should not include an intercept term and contain a maximum of three levels as given by the following code.

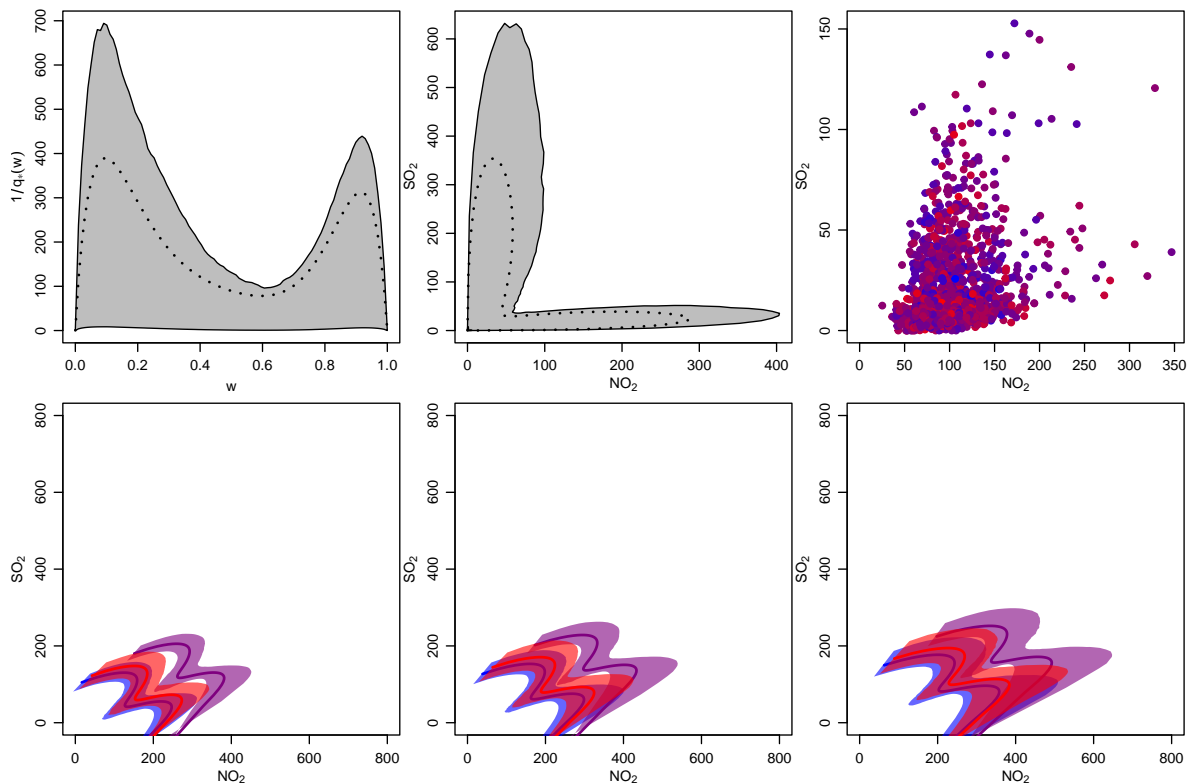


Figure 10: Top row: posterior mean estimate (dotted line) and 90% credible interval (grey) for the inverse of the angular basic density (left), the basic set \mathcal{S} (middle), and observed data (right) with temperature dependent data colouring (from cold = blue to warm = red). Bottom row: posterior mean estimate (dotted line) and 90% credible interval for the extreme bivariate quantiles associated with probabilities $p = 1/600, 1/1200$ and $1/2400$ (left to right) for three maximum daily temperature levels: minimum temperature = blue, median temperature = purple and maximum temperature = red.

```
R> pollut_sum <- summary_ExtDep(mcmc=pollut, burn=5e+3)
R> Temp.seq <- c(min(data[,3]), median(data[,3]), max(data[,3]))
R> QatTemp <- cbind(Temp.seq, Temp.seq^2)
```

We consider representations of quantile regions associated with small probabilities $p = 1/600, 1/1200$ and $1/2400$ and specify that we want to include graphical summaries of the extremal dependence as well as displaying the data (`dep=TRUE` and `data`). The arguments `xlim`, `ylim` and `labels` are graphical parameters for the production of the quantile regions.

```
R> p1 <- plot.ExtDep.np(out=pollut, type="Qsets", summary.mcmc=pollut_sum,
+                       QatCov1=QatTemp, P=1/c(600, 1200, 2400), dep=TRUE,
+                       data=data[, -3], xlim=c(0,800), ylim=c(0,800),
+                       labels=c(expression(NO[2]), expression(SO[2])))
```

The output is stored in the object `p1` which contains a list of dependence quantities in `est.out` and a list of quantile sets in `q.out`. In particular, `est.out` includes the following elements:

- **ghat**: a 3×100 matrix with an estimate of the inverse of the angular basic density q_* evaluated at 100 grid points in $[0, 1]$. Rows gives the posterior 5%-quantile, mean and 95%-quantile.
- **Shat_post** and **Shat**: lists where each element is a 100×2 matrix providing an estimate of the basic set \mathcal{S} (obtained through **ghat**). **Shat_post** considers every posterior samples whereas **Shat** takes the pointwise 5%-quantile, mean and 95%-quantile.
- **nuShat_post** and **nuShat**: two vectors providing the posterior of the basic set measure $\xi(\mathcal{S})$ and its 5%-quantile, mean and 95%-quantile.

The `q.out` list in `pl` includes:

- **Qset_PA_CovNum_B** that is a list of three 100×2 matrices. Each of them is an estimate of the bivariate extreme quantile \tilde{Q}_n . Such regions are computed for the specified probabilities (`P`) and covariate (`QatCov1` and `QatCov2`). E.g., `pl$Qset_P1_CovNum_1` provides an estimate of the (NO_2, SO_2) region corresponding to the probability $1/600$, when the minimum temperature is observed. Each matrix corresponds to the posterior 5%-quantile, mean and 95%-quantile, obtained from `Qset_PA_CovNum_B_post`.
- **Qset_PA_CovNum_B_post** that is a $2 \times (\text{nsim} - \text{burn})$ matrix providing an estimate of the extreme quantile region for each posterior sample.

The argument `dep=TRUE` produces the top row of Figure 10. The bottom row illustrates the extreme quantile regions corresponding to probabilities $1/600$ (left), $1/1,200$ (middle) and $1/2,400$ (right) where the colours indicates different levels of the covariate. Colours of the data (top right), credibility regions and mean from the posterior can be respectively specified by `col.data`, `col.Qfade` and `col.Qfull` (blue to red colour palette by default).

3 Spatial extremes

A convenient tool to statistically model extremes and their dependence over a spatial domain \mathcal{D} is provided by max-stable processes (e.g. [de Haan and Ferreira, 2006](#), Ch. 9). Shortly, let $\{X_i(s), s \in \mathcal{D}\}$, $i = 1, 2, \dots$, be independent copies of a stochastic process $X(s)$, $s \in \mathcal{D}$ with the same finite-dimensional distribution. If there are functions $a_n(s) > 0$ and $b_n(s)$, for each n , such that the finite-dimensional distribution of a limit process $Y(s)$, given by

$$\{Y(s), s \in \mathcal{D}\} = \lim_{n \rightarrow \infty} \left\{ \max_{1 \leq i \leq n} \left(\frac{X_i(s) - b_n(s)}{a_n(s)} \right), s \in \mathcal{D} \right\},$$

is not degenerate, then it must be a multivariate GEV distribution as in (2.2), and with the maximum taken pointwise for all $s \in \mathcal{D}$. Refer to [Davison et al. \(2012\)](#) for a detailed review on max-stable processes and the statistical analysis of spatial extremes. The **ExtremalDep** package considers some of the most widely used max-stable models including the geometric Gaussian ([Davison et al., 2012](#)), the Brown-Resnick ([Brown and Resnick, 1977](#)), the extremal- t ([Opitz, 2013](#)) and the extremal skew- t process ([Beranger et al., 2017](#)). The routines implemented rely on the results of [Dombry et al. \(2016\)](#) and [Beranger et al. \(2021\)](#) for the exact simulation of the max-stable models and on [Stephenson and Tawn \(2005\)](#) and [Beranger et al. \(2021\)](#) for the inferential procedures.

The routine `rExtDepSpat` extends the `rmaxstab` one from the **SpatialExtremes** package (Ribatet, 2022) including exact and direct simulation (`method="direct"` or `"exact"`) from the max-stable process class extremal skew- t , by using the prefix “s” when defining the type of correlation function in the argument `cov.mod` (options are `"whitmat"`, `"cauchy"`, `"powexp"` and `"bessel"`). For the extremal skew- t model, the skewness parameter is represented as

$$\boldsymbol{\alpha} = \alpha_0 + \alpha_1 \mathbf{cov}_1 + \alpha_2 \mathbf{cov}_2 \in \mathbb{R}^d,$$

where \mathbf{cov}_1 and \mathbf{cov}_2 are d -dimensional covariate vectors with d the number of spatial locations $s_j, j = 1, \dots, d$. The argument `alpha` is used to specify $(\alpha_0, \alpha_1, \alpha_2)$ while the covariates are given by `acov1` and `acov2`. In the code below, 50 (`Ny`) replicates of the extremal- t , with $\nu = 1$ degrees of freedom (`DoF`), are generated at 20 (`Ns`) spatial locations (`sites`) in the region $[-5, 5]^2$. The correlation function (`cov.mod`) is the power exponential class $\rho(h) = \exp\{-((\|h\|/r)^\eta)\}$ with smoothness (`smooth`) parameter $\eta = 1.5$ and range (`range`) parameter $r = 3$.

```
R> set.seed(14342)
R> Ns <- 20; Ny <- 50
R> sites <- matrix(runif(Ns*2)*10-5, nrow=Ns, ncol=2)
R> for(i in 1:2) sites[,i] <- sites[,i] - mean(sites[,i])
R> z <- rExtDepSpat(Ny, sites, cov.mod = "tpowexp", DoF = 1, range = 3,
+                 nugget = 0, smooth = 1.5, control = list(method = "exact"))
```

The routine `rExtDepSpat` returns a list consisting of simulated values at specified locations (`$vals`) and the hitting scenario (`$hits`), both being $Ny \times Ns$ matrices. For a given row of `$hits`, elements with the same value indicate block maxima that occurred at the same time (for illustrative purposes one may think that the maxima were obtained from the same “storm”). The `fExtDepSpat` procedure takes advantage of the availability of the time of occurrence of block maxima to fit the extremal- t (`model="ET"`) and skew- t (`model="EST"`) max-stable models using the Stephenson-Tawn likelihood (Stephenson and Tawn, 2005). The correlation function is currently restricted to the power exponential, meaning that the parameters vectors to be estimated are respectively $\theta = (\nu, r, \eta)$ and $\theta = (\nu, r, \eta, \alpha_0, \alpha_1, \alpha_2)$. The corresponding parameters can be fixed through arguments `range`, `smooth`, `DoF` and `alpha` of `fExtDepSpat`. Note that for `alpha`, a vector of length 3 must be provided and therefore a NA value leaves the corresponding parameter free, e.g., `alpha = c(0, NA, NA)` would fit the extremal skew- t model with skewness $\boldsymbol{\alpha} = \alpha_1 \mathbf{cov}_1 + \alpha_2 \mathbf{cov}_2$. Initial values are provided in `par0` in vector form as `c(DoF, range, smooth, alpha0, alpha1, alpha2)`, where fixed or unnecessary parameters are simply omitted. Computations can also be sped-up by considering parallelization (`parallel=TRUE`) and specifying a number of cores (`ncores`) to be used. Arguments `args1` and `args2` are related to specifications of the Monte Carlo simulation scheme to compute the multivariate t cumulative distribution function (cdf). These should take the form of lists including the minimum and maximum number of simulations used (`Nmin` and `Nmax`), the absolute error (`eps`) and whether the error should be controlled on the log-scale (`logeps`). `args1` refers to the $d - 1$ dimensional cdfs terms required to compute the exponent function while `args2` focuses on the $d - m$ ($2 \leq m \leq d - 1$) dimensional cdfs involved in the evaluation of its partial derivatives. When computing the log-likelihood function, the latter terms need to be evaluated on the log-scale, requiring fewer Monte Carlo simulations. In the below, the strategy is to set a higher number of simulations for the partial

derivative terms since experiments have shown that they are more important than the terms in the exponent function (see [Beranger et al., 2021](#)). The `control` argument offers additional control parameters for the optimization algorithm see `?optim` for more details.

```
R> args1 <- list(Nmax=50L, Nmin=5L, eps = 0.001, logeps = FALSE)
R> args2 <- list(Nmax=500L, Nmin=50L, eps = 0.001, logeps = TRUE)
R> fit1 <- fExtDepSpat(model="ET", z=z$vals, sites=sites, hit=z$hits,
+                     par0=c(3,1,1), parallel=TRUE, ncores=6,
+                     args1=args1, args2=args2, control = list(trace=0))
R> fit1$est
```

```
      DoF   range  smooth
1.061558 3.025641 1.462166
```

The routine `fExtDepSpat` returns a list including the estimated parameters (`$est`), the dimensionality of the joint density (`$jw`), the value of the maximised log-likelihood (`$LL`), the standard errors computed from the sandwich information matrix (`$stderr.sand`) and the Takeuchi Information Criteria (`$TIC`). In the above, the estimated parameter vector is $\hat{\theta} = (1.06, 3.03, 1.46)$, while the true parameters are $\theta = (1, 3, 1.5)$. In addition, `est1$jw` takes value 20 indicating that the full likelihood was considered (default). As proposed in [Beranger et al. \(2021\)](#), composite likelihood estimation ([Padoan et al., 2010](#)) is incorporated when the argument `jw` is specified and is less than the number of locations. Since the number of tuples (pairs if `jw=2`, triples if `jw=3`) is increasing with `jw` one can specify a threshold u through the argument `thresh` such that, for a tuple q , the corresponding composite likelihood contribution is weighted according to

$$w_q = \begin{cases} 1 & \text{if } \max_{i,k \in q; i \neq k} \|s_i - s_k\| < u \\ 0 & \text{otherwise} \end{cases}.$$

In other words, only tuples with maximum pairwise distance less than u are included in the likelihood.

```
R> fit2 <- fExtDepSpat(model="ET", z=z$vals, sites=sites, hit=z$hits,
+                     par0=c(3, 1, 1), thresh = quantile(dist(sites), 0.25),
+                     jw=3, parallel=TRUE, ncores=6,
+                     args1=args1, args2=args2, control = list(trace=0))
R> fit2$est
```

```
      DoF   range  smooth
1.163204 3.487388 1.450581
```

The above code fits the extremal- t model using the triplewise composite-likelihood approach with threshold u set at the first quartile of pairwise distances. The estimated parameter vector is $\hat{\theta} = (1.16, 3.49, 1.45)$, which is again close to the true one $\theta = (1, 3, 1.5)$.

We now analyze temperature data around Melbourne, Australia, collected at 90 stations on a 0.15 degree (approximately 13 kilometer) grid in a 9 by 10 formation, over the extended summer period from August to April between 1961 and 2010. Running the command `data(heat)` loads several important datasets in **R**. The objects `locgrid`, `scalegrid` and

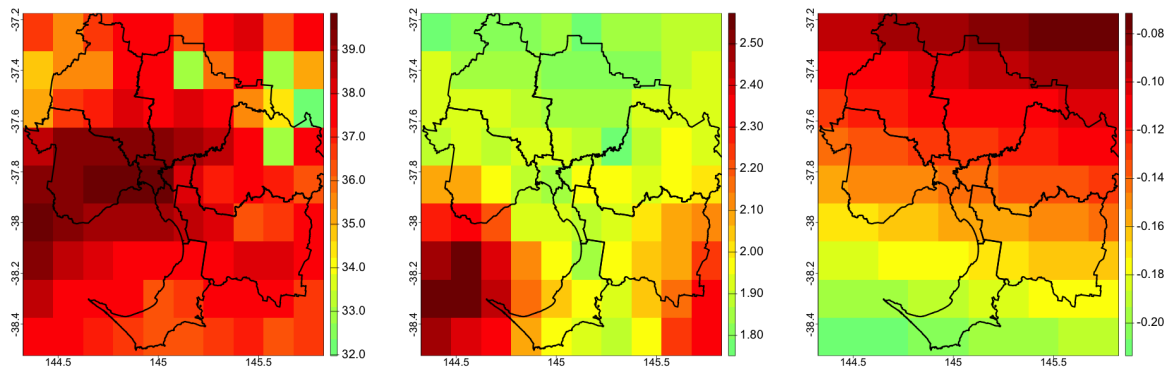


Figure 11: Estimated marginal location (left), scale (middle) and shape (right) parameters.

`shapegrid` are matrices of the marginal GEV parameters estimated over the grid using unconstrained location and scale while the shape parameter is defined as a linear function of eastings and northings in 100 kilometer units. In the following code, the `terra` package (Hijmans, 2024) is used to provide graphical illustrations of these objects.

```
R> library(terra)

R> data(heat)
R> path <- "https://www.abs.gov.au/statistics/standards/australian-statistical-
geography-standard-asgs-edition-3/jul2021-jun2026/access-and-
downloads/digital-boundary-files"
R> file.name <- "SA4_2021_AUST_SHP_GDA2020.zip"
R> download.file(file.path(path, file.name), destfile=file.name)
R> unzip(file.name)
R> geogmel <- vect("SA4_2021_AUST_GDA2020.shp")
R> geogmel <- geogmel[geogmel$GCC_NAME21 == "Greater Melbourne"]
R> unlink(list.files(pattern = "SA4_2021_AUST"))

R> lat <- seq(from=-38.45, by=0.15, length=9)
R> lon <- seq(from=144.4, by=0.15, length=10)
R> xx <- expand.grid(lon=lon, lat=lat)
R> cols <- tim.colors(40)[20:40]
R> for(m in c("locgrid", "scalegrid", "shapegrid")){
+   mat <- mget(m)
+   xx$data <- as.vector(mat[[1]])
+   rd <- rast(xx, crs=crs(geogmel))
+   plot(rd, col=cols, plg= list(cex=2),pax=list(cex.axis=2))
+   lines(geogmel,lwd=3)
+ }
```

Note that the code first downloads shape files and extracts the Greater Melbourne region. Also provided in `heat` is the object `heatdata` which is a list with elements:

- `vals`: the 50 yearly maxima (rows) at each of the 90 locations (columns)

- `ufvals`: `vals` marginally transformed to unit-Fréchet scale
- `hits`: the hitting scenarios for each year (row) and location (row). Locations with the same integer value correspond to maxima obtained on the same day (± 3 days).
- `sitesLLO`, `sitesENO`: original location coordinates in latitude-longitude (LL) and easting-northing (EN, in kilometer)
- `sitesLL`, `sitesEN`: same as `sitesLLO`, `sitesENO` but centered.

Next, the extremal skew- t model with $\nu = 5$ is fitted to the data. Since the observations were marginalized with GEV shape parameter as function of eastings and northings in 100 kilometer units, the site locations are transformed to be on the same scale. Note that [Beranger et al. \(2021\)](#) used the TIC for model selection between the extremal- t and extremal skew- t with $\nu = 1, 3$ and 5 degrees, but here for simplicity we only consider the selected model.

```
R> z <- heatdata$ufvals; hits <- heatdata$hits
R> sites <- heatdata$sitesEN/100
R> args1 <- list(Nmax=20L, Nmin=2L, eps = 0.001, logeps = FALSE)
R> args2 <- list(Nmax=200L, Nmin=20L, eps = 0.001, logeps = TRUE)

R> est5 <- fExtDepSpat(model="EST", z=z, sites=sites, hit=hits,
+                    par0=c(et1$est, 0, 0, 0), DoF=5, acov1 = sites[,1],
+                    acov2 = sites[,2], parallel=TRUE, ncores=6,
+                    args1 = args1, args2 = args2, control = list(trace=2))
R> est5$est

      range      smooth   alpha.0   alpha.1   alpha.2
11.5011962  1.1692750  0.1444647 -0.3520854 -0.7790411
```

The estimated range and smoothness of the skew- t are respectively $\hat{r} = 11.50$, $\hat{\eta} = 1.17$, while the skewness is estimated as $\hat{\alpha} = 0.14 - 0.35$ easting $- 0.78$ northing. The largest distance between pairs of locations (in 100 kilometer units) is 1.785, and therefore the smallest correlation is $\exp\left[-(1.785/\hat{r})^{\hat{\eta}}\right] \approx 0.89$, indicating a strong degree of spatial dependence. Finally, the `rExtDepSpat` function is used to simulate from the extremal skew- t conditionally on the hitting scenario and Figure 12 displays an example conditioning on at most two heatwave events causing the annual maxima.

```
R> set.seed(123)
R> while(TRUE){
+   z.new <- rExtDepSpat(1, sites, cov.mod = "spowexp", DoF = 5, nugget = 0,
+                       range = est5$est[1], smooth = est5$est[2],
+                       alpha = est5$est[3:5], acov1 = sites[,1],
+                       acov2 = sites[,2], control = list(method = "exact"))
+   if(length(unique(as.numeric(z.new$hits))) <= 2) break
+ }

R> parmat <- cbind(as.vector(locgrid), as.vector(scalegrid), as.vector(shapegrid))
R> z.new.GEV <- matrix(trans2GEV(data=z.new$vals, pars=parmat), nrow=nrow(locgrid))
```

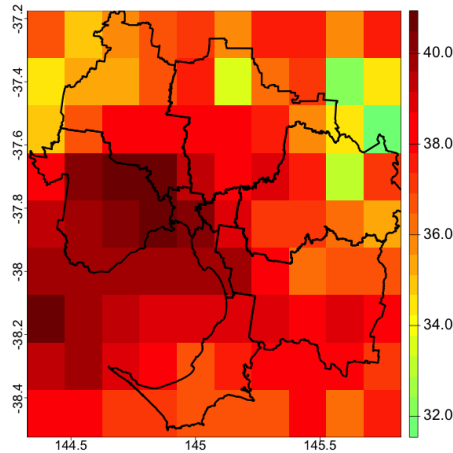


Figure 12: Simulation from the fitted extremal skew- t model with $\nu = 5$, conditioning on at most two heatwave events causing all maxima.

```
R> xx$data <- as.vector(z.new.GEV)
R> rd <- rast(xx, crs=crs(geogmel))
R> plot(rd, col=cols, plg= list(cex=2),pax=list(cex.axis=2))
R> lines(geogmel,lwd=3)
```

Acknowledgements

BB is supported by the Australian Research Council through the Discovery Project Scheme (DP220103269). SP is supported by the Bocconi Institute for Data Science and Analytics (BIDSA) and project MUR - Prin 2022 - Prot. 20227YZ9JK, Italy.

References

- Beirlant, J., Y. Goegebeur, J. Segers, and J. L. Teugels (2004). *Statistics of extremes: theory and applications*. John Wiley & Sons.
- Belzile, L. R., C. Dutang, P. J. Northrop, and T. Opitz (2023). A modeler’s guide to extreme value software. *Extremes* 26(4), 595–638.
- Belzile, L. R., S. D. Grimshaw, R. Huser, P. J. Northrop, and J. L. Wadsworth (2022). *mev: Modelling of Extreme Values*. R package version 1.17.
- Beranger, B. and S. Padoan (2015). Extreme dependence models. In *Extreme Value Modeling and Risk Analysis*, pp. 325–352. Chapman and Hall/CRC.
- Beranger, B., S. A. Padoan, and G. Marcon (2024). *ExtremalDep: Extremal Dependence Models*. R package version 0.0.4-2.
- Beranger, B., S. A. Padoan, and S. A. Sisson (2017). Models for extremal dependence derived from skew-symmetric families. *Scandinavian Journal of Statistics* 44(1), 21–45.

- Beranger, B., S. A. Padoan, and S. A. Sisson (2021). Estimation and uncertainty quantification for extreme quantile regions. *Extremes* 24(2), 349–375.
- Beranger, B., A. G. Stephenson, and S. A. Sisson (2021). High-dimensional inference using the extremal skew-t process. *Extremes* 24(3), 653–685.
- Bernard, E., P. Naveau, M. Vrac, and O. Mestre (2013). Clustering of maxima: Spatial dependencies among heavy rainfall in france. *Journal of climate* 26(20), 7929–7937.
- Brown, B. M. and S. I. Resnick (1977). Extreme values of independent stochastic processes. *J. Appl. Probability* 14(4), 732–739.
- Cai, J.-J., J. H. Einmahl, and L. De Haan (2011). Estimation of extreme risk regions under multivariate regular variation. *The Annals of Statistics* 39(3), 1803–1826.
- Coles, S. (2001). *An introduction to statistical modeling of extreme values*. Springer.
- Coles, S. G. and J. A. Tawn (1991). Modelling extreme multivariate events. *Journal of the Royal Statistical Society: Series B (Methodological)* 53(2), 377–392.
- Cooley, D., R. A. Davis, and P. Naveau (2010). The pairwise beta distribution: a flexible parametric multivariate model for extremes. *J. Multivariate Anal.* 101(9), 2103–2117.
- Cormier, E., C. Genest, and J. G. Nešlehová (2014). Using b-splines for nonparametric inference on bivariate extreme-value copulas. *Extremes* 17(4), 633–659.
- Davis, R. A., T. Mikosch, and I. Cribben (2011). Estimating extremal dependence in univariate and multivariate time series via the extremogram. <https://arxiv.org/abs/1107.5592>.
- Davison, A., S. Padoan, and M. Ribatet (2012). Statistical modeling of spatial extremes, with discussion. *Statistical Science* 27(2), 161–186.
- de Fondeville, R. and L. R. Belzile (2021). *mvPot: Multivariate peaks-over-threshold modelling for spatial extreme events*. R package version 0.1.5.
- de Fondeville, R. and A. C. Davison (2018). High-dimensional peaks-over-threshold inference. *Biometrika* 105(3), 575–592.
- de Haan, L. and A. Ferreira (2006). *Extreme value theory: an introduction*, Volume 21. Springer.
- Dombry, C., S. Engelke, and M. Oesting (2016). Exact simulation of max-stable processes. *Biometrika* 103(2), 303–317.
- Einmahl, J. H., L. de Haan, and A. Krajina (2013). Estimating extreme bivariate quantile regions. *Extremes* 16(2), 121–145.
- Engelke, S. and A. S. Hitz (2020). Graphical models for extremes. *Journal of the Royal Statistical Society: Series B* 84(4), 871–932.
- Engelke, S., A. S. Hitz, N. Gnecco, and M. Hentschel (2024). *graphicalExtremes: Statistical Methodology for Graphical Extreme Value Models*. R package version 0.3.2.

- Engelke, S., A. Malinowski, Z. Kabluchko, and M. Schlather (2015). Estimation of hüsler–reiss distributions and brown–resnick processes. *Journal of the Royal Statistical Society: Series B (Statistical Methodology)* 77(1), 239–265.
- Falk, M., J. Hüsler, and R.-D. Reiss (2010). *Laws of small numbers: extremes and rare events*. Springer Science & Business Media.
- Fils-Villetard, A., A. Guillou, and J. Segers (2008). Projection estimators of pickands dependence functions. *Canadian Journal of Statistics* 36(3), 369–382.
- Frolova, N. and I. Cribben (2016). *extremogram: Estimation of Extreme Value Dependence for Time Series Data*. R package version 1.0.2.
- Garthwaite, P. H., Y. Fan, and S. A. Sisson (2016). Adaptive optimal scaling of metropolis–hastings algorithms using the robbins–monro process. *Communications in Statistics-Theory and Methods* 45(17), 5098–5111.
- Gilleland, E. and R. W. Katz (2016). extremes 2.0: An extreme value analysis package in R. *Journal of Statistical Software* 72(8), 1–39.
- Haario, H., E. Saksman, and J. Tamminen (2001). An adaptive Metropolis algorithm. *Bernoulli* 7, 223–242.
- He, Y. and J. H. Einmahl (2017). Estimation of extreme depth-based quantile regions. *Journal of the Royal Statistical Society: Series B (Statistical Methodology)* 79(2), 449–461.
- Heffernan, J. E. and A. G. Stephenson (2018). *ismev: An introduction to statistical modeling of extreme values*. R package version 1.4.2.
- Heffernan, J. E. and J. A. Tawn (2004). A conditional approach for multivariate extreme values (with discussion). *Journal of the Royal Statistical Society: Series B (Statistical Methodology)* 66(3), 497–546.
- Hijmans, R. J. (2024). *terra: Spatial Data Analysis*. R package version 1.7-78.
- Joe, H. (2014). *Dependence modeling with copulas*. CRC press.
- Marcon, G., P. Naveau, and S. Padoan (2017). A semi-parametric stochastic generator for bivariate extreme events. *Stat* 6(1), 184–201.
- Marcon, G., S. A. Padoan, and I. Antoniano-Villalobos (2016). Bayesian inference for the extremal dependence. *Electronic Journal of Statistics* 10(2), 3310–3337.
- Marcon, G., S. A. Padoan, P. Naveau, P. Muliere, and J. Segers (2017). Multivariate non-parametric estimation of the Pickands dependence function using Bernstein polynomials. *J. Statist. Plann. Inference* 183, 1–17.
- Northrop, P. J. and N. Attalides (2016). Posterior propriety in bayesian extreme value analyses using reference priors. *Statistica Sinica* 26(2), 721–743.
- Opitz, T. (2013). Extremal t processes: Elliptical domain of attraction and a spectral representation. *Journal of Multivariate Analysis* 122(0), 409 – 413.

- Padoan, S. A., M. Ribatet, and S. A. Sisson (2010). Likelihood-based inference for max-stable processes. *Journal of the American Statistical Association* 105(489), 263–277.
- Padoan, S. A. and G. Stupfler (2020). *ExtremeRisks: Extreme risk measures*. R package version 0.0.4.
- Ribatet, M. (2022). *SpatialExtremes: Modelling Spatial Extremes*. R package version 2.1-0.
- Roberts, G. O., A. Gelman, and W. R. Gilks (1997). Weak convergence and optimal scaling of random walk Metropolis algorithms. *Annals of Applied Probability* 7(1), 110–120.
- Sabourin, A., P. Naveau, and A.-L. Fougères (2013). Bayesian model averaging for multivariate extremes. *Extremes* 16(3), 325–350.
- Stephenson, A. and J. Tawn (2005). Exploiting occurrence times in likelihood inference for componentwise maxima. *Biometrika* 92(1), 213–227.
- Stephenson, A. G. (2002, June). evd: Extreme value distributions. *R News* 2(2), 31–32.
- Stephenson, A. G. and M. Ribatet (2023). *evdbayes: Bayesian Analysis in Extreme Value Theory*. R package version 1.1-3.
- Ypma, J. and S. G. Johnson (2022). The nlopt nonlinear-optimization package. R package version 2.0.3.